SURVEY

A Review on Through-Wall Communications: Wall Characterization, Applications, Technologies, and Prospects

HOJJAT JAMSHIDI-ZARMEHRI [1], (Graduate Student Member, IEEE), **AMIR AKBARI** [1], **MOHAMMAD LABADLIA** [1], **KAM EUCHARIST KEDZE** [1], **JAFAR SHAKER** [1], (Senior Member, IEEE), **GAOZHI XIAO** [2], (Fellow, IEEE), AND **RONY E. AMAYA** [1], (Senior Member, IEEE)

[1] Department of Electronics, Carleton University, Ottawa, ON K1S 5B6, Canada
[2] Advanced Electronics and Photonics Research Center, National Research Council (NRC) Canada, Ottawa, ON K1A 0R6, Canada

Corresponding author: Hojjat Jamshidi-Zarmehri (hojjatjamshidizarmeh@cmail.carleton.ca)

ABSTRACT This paper underscores the paramount significance of through-wall communications by providing a comprehensive exploration of pivotal aspects like wall characterization, relevant technologies, versatile applications, and future prospects. Through-wall communication has the potential of being adopted in diverse fields, from indoor wireless communications, ground penetrating radar, through-wall radar imaging, to even power transmission. To augment the efficiency and reliability of signal detection, a whole variety of tools, such as antenna elements, frequency-selective structures, metasurfaces, and lenses, are exploited. By surveying the landscape of relevant technologies and applications in the existing literature, this paper serves as a beacon for researchers and engineers alike. Furthermore, it extends an invitation for pioneering exploration in this field, advocating the examination of tunable and adaptive systems, as well as the untapped potential of 3D printing in reshaping the future of through-wall communications.

INDEX TERMS Antenna arrays, bow-tie antennas, frequency selective structures (FSSs), ground penetrating radar (GPR), horn antennas, indoor communications, lenses, metamaterials, metasurfaces, microstrip antennas, power transfer, through-wall communications (TWC), through-wall power transfer (TWPT), through-wall radar imaging (TWRI), Vivaldi antennas.

I. INTRODUCTION

The objective of through-wall communication (TWC) is the transmission of electromagnetic waves in the form of data and/or power to the other side of an obstacle. Due to dielectric material losses, penetrating electromagnetic waves in walls is challenging. On the other hand, the frequency dependence of this loss poses challenges for TWC in frequency bands with high dielectric loss [1], [2], [3], [4], [5], [6], [7].

Furthermore, wall thickness and dielectric constant do not have well-established values, which would degrade the resolution in imaging radar systems [8]. A potential solution to

The associate editor coordinating the review of this manuscript and approving it for publication was Vishal Srivastava.

overcome these challenges would be raising the power level of propagating waves to guarantee signal reliability. However, due to health concerns, the signal power cannot exceed a particular value [9]. This value is determined based on operation frequency, the part of the body that is exposed, and Specific Absorption Rate (SAR) (the amount of RF energy absorbed by tissues in the human body). Institute of Electrical and Electronic Engineers (IEEE) [10] and International Commission on Non-Ionizing Radiation Protection (ICNIRP) [11] provide guidelines for power levels considering the safety of humans in the environment.

Through-wall communication is employed in many applications like indoor propagation [12], [13], [14], [15], [16], [17], ground penetration radars (GPR) [18], [19], [20], [21], [22], through-wall imaging radars (TWIR) [23], [24], [25],

[26], [27], [28], [29], [30], [31], [32], and power transmission through walls [33], [34], [35], [36], [37], [38], [39].

Stable signal coverage in indoor environments, including walls and other materials, is essential for indoor communications. With the introduction of the Internet of Things (IoT) and smart houses, electromagnetic waves with different operation frequencies propagate in buildings [17], [40], [41]. In these environments, through-wall communication aims to improve the reliability of the signal.

Transmission of power through walls is another branch of TWC which has been investigated in literature [42], [43], [44], [45], [46], [47]. Inductive [36], capacitive [34], [48], and magnetic coupling [49] methods are some common approaches which allow the transmission of power through metallic or dielectric walls.

Furthermore, Through-wall microwave imaging is used to detect targets and humans on the other side of a wall or other dielectric materials. Ultra-wideband (UWB) antennas are an essential part of a through-wall imaging system. Some methods like Scale-Adaptive Human Target Tracking [23] and Hybrid FT-MUSIC Technique [50] are used to process the reflected waves for detection. Ground penetration radars are also a part of the imaging systems, aiming to detect underground objects [19].

Regarding the technologies, improving antenna performance has been a popular method to increase the reliability and power of the signal behind a wall. The most popular antennas for through-wall applications include Vivaldi [22], [29], [51], [52], [53], [54], horn [55], bow tie [56], [57], and microstrip patch [53], [58], [59], [60], [61] antennas. However, other antennas like magneto-electric dipoles [62], [63], and tapered slot [64], [65], [66] antennas are also utilized for through-wall and GPR applications. Antenna arrays using SIW technology [67], patch antennas [68], [69], [70], Vivaldi antennas [71], [72], [73], and tapered slot antennas [74] are also recommended to improve the radiation gain of the system.

Another technology that can be applied in combination with antennas is frequency selective surfaces (FSSs) [75], [76], [77], [78]. FSSs are periodic planar structures that consist of metallic surfaces on dielectric substrates [79], [80]. They can be employed in either transmission or reflection modes depending on the design frequency [81]. Therefore, FSSs can be considered spatial filters which allow electromagnetic waves to be transmitted/blocked in designated frequency bands [82], [83]. This property can improve the selectivity in through-wall applications to introduce smart walls and windows [13], [14], [15], [16], [84], [85], improve the gain of antennas [70], and signal enhancement for indoor applications [86], [87], [88], [89].

Metamaterials and metasurfaces have also drawn attention to improve the systems' performance for through-wall applications [24], [90], [91]. The design of metamaterials, which are considered materials with effective permittivity and permeability that cannot be found in nature, has been a topic of intense research in the last few decades. Metamaterials have been used in the design of antennas [92], [93], [94], absorbers [95], imagers [96], and other microwave components [97], [98], [99], [100] to improve the radiation and guiding characteristics of the designs.

Metasurfaces are periodic structures that can be characterized through their equivalent surface impedance and electric and magnetic polarizabilities [101]. These structures have been utilized in antennas for sidelobe suppression [102], tunability [103], and mantle cloaking [104]. They have been also employed in polarization converters [105] and a wide variety of other microwave applications [106], [107], [108].

Lenses are another approach that can increase the signal coverage and power in through-wall communications systems. Metalenses with ultrathin films that are employed on the walls can improve signal strength in indoor communications [109]. Dielectric lenses can also be used as an add-on structure to radiating elements, improving the system's radiating gain [109], [110]. This method allows more efficient penetration of electromagnetic fields into dielectric materials.

In this paper, a review of wall characterization, applications, and technologies related to through-wall communications is presented. There are surveys that are dedicated to a particular aspect of through-wall communications such as: imaging systems [31], power transfer through walls [37], or antennas [19], [66], [90]. However, this paper, for the first time, has tried to cover all aspects of through-wall communications, including the effects of walls, typical applications, and relevant and promising technologies. In addition, the paper offers new prospects for future studies.

Throughout this manuscript, walls refer to dielectric materials, which include bricks, concrete, soil, and/or other materials with similar properties. Metal walls are not included in this paper since the behaviour of the electromagnetic waves in metallic walls would be different.

The organization of the paper is as follows. In section II, wall parameters and characterization are reported. Different applications containing indoor communication, imaging, and power transmission are briefly discussed in section III. Section IV reviews some technologies which are commonly used for through-wall communications. Moreover, prospects for future research are recommended in section V, followed by a conclusion in section VI.

II. WALL CHARACTERIZATION

In through-wall communications, it is crucial to understand the structure, electrical properties, and other aspects of the walls to increase wireless coverage and reliability. These can help to improve signal efficiency in through-wall applications [111], [112], [113].

In most applications, including indoor communication and through-wall imaging, walls refer to building walls made using brick, concrete, wood, glass, chipboard, and plasterboard. The dielectric properties of these materials have been reported in Table 1. However, in general, walls can

be constructed using different materials, including the cited materials and metallic parts. Wall parameters are important in indoor environments since the amount of attenuation can affect the link's reliability. Fig.1 (a) shows a wall which blocks Wi-Fi signals in a building.

Fig.1 (b) shows a GPR system where the ground can be considered an infinite wall. Furthermore, in some GPR applications, like measuring the thickness and density of asphalt for quality monitoring, the wall can be other materials. Table 2 summarizes the dielectric constant and propagation velocity within commonly used materials that are most relevant in GPR systems.

TABLE 2. The dielectric constant and propagation velocity of different materials in GPR systems [118], [119].

Material	ε_r	Propagation velocity (m/ns)
Ice (Frozen soil)	4	0.15
Granite	9	0.10
Limestone	6	0.12
Sandstone	4	0.15
Dry sand	2 - 6	0.12 - 0.15
Wet sand	30	0.055
Dry clay	8	0.11
Wet clay	33	0.052
Asphalt	3 - 6	0.12 - 0.17
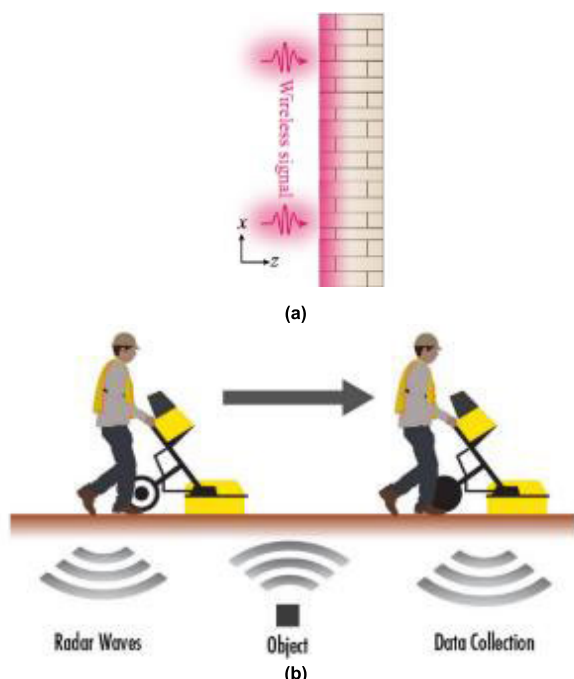
FIGURE 1. a) Wall in indoor and through-wall imaging systems [109] b) ground as an infinite wall in GPR applications [114].

TABLE 1. The complex dielectric constant of different materials used in building walls [115], [116], [117].

Material	ε_r	Loss tangent
Concrete	3-6	0.012-0.032
Brick wall	3-5	0.095
Plasterboard	2-2.5	0.026-0.1
Wood	2-3	0.14-0.3
Glass	5.5-6.5	0.17-0.18
Chipboard	2-3	0.17-0.78
Drywall	2.8	-

In addition, in some applications, like through-wall radar imaging, the estimation of wall parameters, including dielectric constant, loss tangent, thickness, and conductivity, would be critical. Extracting these parameters can help to obtain

precise results for detection purposes. An erroneous estimate compromises the quality of the reconstructed image [8] [120], [121]. Different methods have been introduced in the literature for wall characterization [122], [123], [124], [125], [126], [127]. In most cases, measurement/calculation of S-parameters is used for extracting the wall properties.

Many time-domain reflectometry-based estimation methods were put out in [128], [129], [130], [131]. While the reflectometry technique can produce precise estimates, its constrained bandwidth and resolution can occasionally render it challenging to discriminate between several reflections in the time domain. The inverse fast Fourier transform (IFFT) is frequently used to convert frequency-domain measurements into time-domain data to bypass rather commercial time-domain measurement equipment that is complex and expensive. However, this conversion procedure may obscure the frequency response of wall material parameters.

Therefore, the development of a frequency-domain algorithm that does not require further analysis is of great significance. A frequency-domain approach has been introduced in [128] for calculating wall parameters that minimizes the discrepancy between experimental and analytical reflection coefficients using the least squares minimization method. However, a first approximation of the wall parameters is derived using time-domain reflectometry to reduce computational complexity. This strategy, however, is prone to non-unique solutions and trapping in local minima, which is a general limitation of the least squares minimization process.

Another algorithm was also developed in [132] based on S-parameters and pole extraction to obtain the properties of multi-layered walls in through-wall imaging systems. The approach employed in this technique involves utilizing the generalized pencil of functions (GPOF) method to establish a connection between the complex S-parameter and the wall parameters. Unlike traditional methods that rely on IFFT to retrieve time-domain data, this technique leverages the extraction of frequency response poles of the medium. By doing so, it enables the determination of essential wall parameters such as the complex permittivity and thickness of each layer in the wall. Additionally, a precise

calibration technique is introduced to account for the physical antenna frequency response, allowing the observed frequency response to match the extraction formulation. The calibration technique is derived from a forward scattering problem model. Fig. 2 shows the experimental setup for wall characterization.
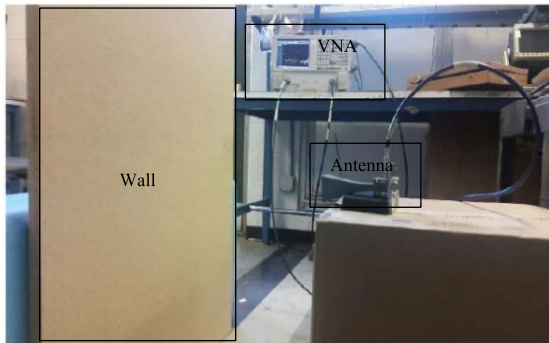

FIGURE 2. The measurement setup for the characterization of a multi-layered wall [132].

A comparison between some methods for wall characterization is presented in Table 3. The error of the estimated parameters from the actual ones is also reported in this Table. It can be seen that the method presented in [132] provides more reliable results compared with FFT-based algorithms.

TABLE 3. A comparison between the estimated and actual parameters of the wall using different methods.

Reference	Distance (cm)		Permittivity		Thickness (cm)	
	actual	error (%)	actual	error (%)	actual	error (%)
[132]	-	-	6	1.3	20	0.25
[131]	-	-	7	2.1	14.5	0.8
[133]	-	-	7.66	6	20	5.5
[135]	42	0.09	Multi-layered	-	4.46	0.2

III. APPLICATIONS

In this section, some typical applications of through-wall communications are introduced. To the best of our knowledge, the main through-wall applications include indoor communications, power transfer through the wall, and imaging. A brief description of each application is summarized in this part.

A. INDOOR COMMUNICATIONS

A typical application of through-wall communications is in buildings where the amplitude of the signal should be improved for reliable links. Electromagnetic waves can propagate through multipaths. The received signal can be a combination of reflections, refractions, diffractions, and scattering of the transmitted waves. Depending on the path loss,

these signals can be combined in phase or out of phase, making the amplitude of the received signal variable [40], [112], [113]. As a result of reflections and transmissions through building materials, a typical indoor environment attenuates the received signal. Different factors affect the building penetration loss, including but not limited to a building's structure and the material used in the walls [4], [5], [6], [111].

Modelling of walls and other obstacles in indoor communication to predict the behaviour of electromagnetic waves has been investigated to improve signal reliability in indoor environments [111], [133], [134]. In addition, these models can be used to enhance the electromagnetic features of the buildings.

In [116] a frequency-selective wall and external modules are presented to improve the signal coverage inside buildings. Fig. 3 (a) and (b) show the smart brick and the external module, respectively. Smart bricks can be replaced with typical bricks, while external modules should be employed on normal walls.
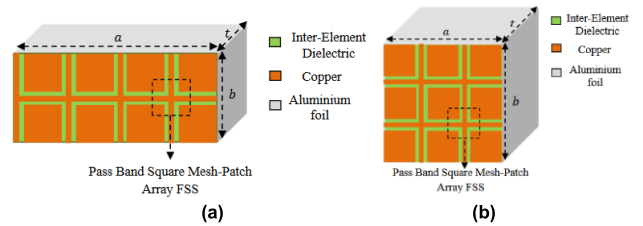

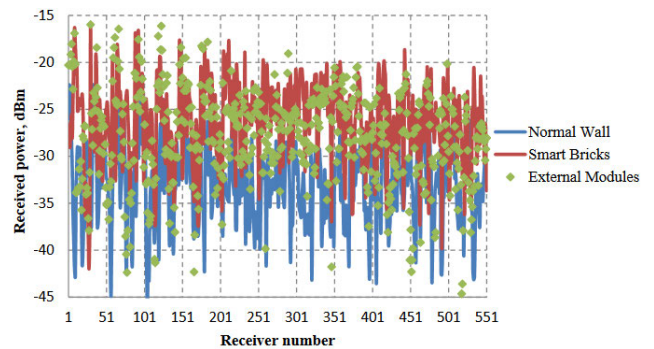**FIGURE 3.** a) Smart brick b) external module, using FSS [116].

FIGURE 4. The measured received power in the building for normal walls, smart walls, and walls with external modules [116].

The structures contain a common square loop FSS on the side face and conductor in the tops and edges of the brick. The smart brick is filled by regular brick ($\varepsilon_r = 4.44$), but the external module is filled with air ($\varepsilon_r = 1$). The measured power in the building for both smart wall and external modules in comparison with the normal wall is illustrated in Fig. 4. It can be seen that a power enhancement of about 10 dB, and 5 dB (on average) is achieved when smart bricks and external modules are used, respectively.

Millimeter-wave indoor communications encompass a broad frequency spectrum ranging from 30 GHz to 300 GHz,

presenting exciting prospects for leveraging this range for high-speed broadband applications. Utilizing appropriate modulation and coding schemes within the framework of the IEEE 802.11ad standard designed for 60 GHz indoor communications, a maximum data rate of 6.756 Gbps can be achieved [135]. This achievement has ignited increased interest in exploring other frequencies within the millimeter-wave spectrum, specifically in the frequency bands spanning 28–38 GHz and 70–90 GHz [136].

Table 4 shows a typical link budget scenario for indoor wireless personal area network (WPAN) uplink millimetre-wave systems to highlight the significance of antenna gain in millimetre-wave indoor communications [136]. To attain an acceptable bit error rate (BER) for demodulating quadrature phase shift keying (QPSK) signals, a receiver's signal-to-noise ratio (SNR) must be at least 10 dB. This is taken into consideration while determining system link margins. It becomes clear that the construction of a practical and long-lasting millimetre-wave communication link depends on the efficiency of transmit and receive antenna gains, given the significant propagation loss inherent in these applications.

TABLE 4. Required system link budget for a typical indoor communication system [136].

| Parameter	Value
Carrier Frequency (GHz)	60
Max. Range (m)	10
Bandwidth (GHz)	2
Transmit Power (dBm)	10
Propagation Loss (dB)	-88
Implementation Loss (dB)	-5
Thermal PSD (dBm/Hz)	-174
Rx Noise Figure (dB)	10
Rx Thermal Noise (dB)	-71
Receiver SNR (dB)	-12
Required SNR (QPSK) (dB)	10
System Margin (dB)	-22
Transmit Antenna Gain (dBi)	20
Receive Antenna Gain (dBi)	10
System Margin (dB) with Tx and Rx antenna gains	8

The performance of indoor millimetre-wave communication in the presence of multipath interference is notably enhanced through the utilization of directional antennas. In [137], Employing a ray tracing approach supported by propagation measurements, simulations yield a root-mean-squared (RMS) delay spread below 5 ns. An exploration

into the impact of polarization is also conducted in [138], revealing that the joint utilization of directional antennas and circular polarization leads to a halving of the multipath spread.

In the realm of indoor WPAN, the introduction of spatial reuse mode via beamforming utilizing steerable antennas with eight parallel communication links results in a 3–5 times increase in overall millimetre-wave WPAN system throughput compared to traditional time division mode [139]. Addressing robustness against line-of-sight (LOS) blockages is a compelling research domain, where antenna beamforming is anticipated to assume a pivotal role [140], [141], [142].

B. POWER TRANSMISSION

Transferring power through walls has been an interesting research area under development. One method to transfer power to another side of a wall is inductive power transfer (IPT). This method is the most common method for power transferring [37]. Fig. 5 illustrates a schematic view and experimental setup of through-wall wireless power transfer using an inductive coupling system introduced in [36]. Metal coils have been used in this structure to transfer power.
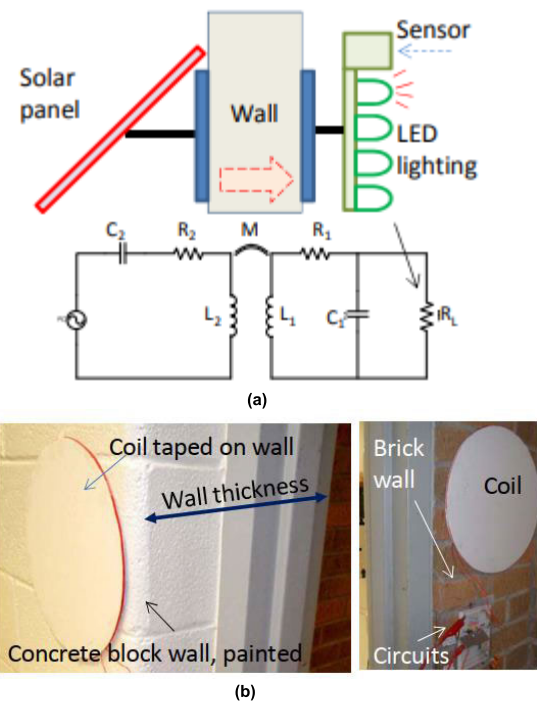
FIGURE 5. a) The configuration of a system for transferring power through the wall with an equivalent circuit b) the experimental setup [36].

This system can wirelessly transfer power from external sources like solar panels, wind turbines, and hydraulic sources into a building. In this design, the energy source employs an oscillator in conjunction with an amplifier to produce a radio frequency (RF) signal. Matching between the resonant circuit and the amplifier affects the level of power

transmitted through the wall. The carrier frequency and the load have been 1.3 MHz and 500 ohms, respectively.

The efficiency and output power results versus matching capacitance are also illustrated in Fig. 6. The results for two different spacing thicknesses of 4.4 cm and 8.5 cm have been reported. It can be seen that maximum output power and maximum efficiency are different matching points. Matching capacitance can be tuned to obtain the best point for maximum output power.

In addition to inductive power transfer, other methods like capacitively coupled power transfer (CCPT) based on electric field coupling [34], [48], and magnetic resonant coupling [38], [49] can also be used for transferring power through metallic or dielectric walls.
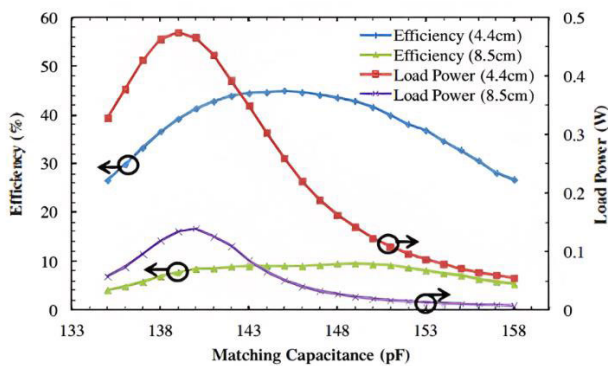
FIGURE 6. The output power and efficiency results versus matching capacitance for two different spacing thicknesses [36].

C. THROUGH-WALL IMAGING

Several industries are interested in imaging through dielectric materials, including rescue missions, medical imaging, and security surveillance. In order to figure out the distribution of materials, electromagnetic waves are transmitted toward objects, and the resulting scattered field is measured by given techniques as outlined in [23], [25], [32], and [143]. These systems can help to find concealed objects or humans in the ground or behind the walls [23], [24], [144], [145].

Despite the dielectric properties of brick walls, drywall, and even concrete, millimetre waves can penetrate through these materials. With increased bandwidth, high-resolution images can be captured to increase the possibility of detecting and tracking objects on the other side of the wall. The allocated operation frequency by International Telecommunication Union (ITU) for UWB through-wall applications is between 1.99 GHz and 10.6 GHz [9].

In addition, the technologies applied for through-wall imaging should have high and stable gain in the operation bandwidth [54]. They should also have stable radiation patterns over the operating frequency and wide impedance bandwidth to improve the resolution. Low profile, low cost, and planar structures are other requirements that make the system a good option for integration with monolithic microwave-integrated circuits (MMICs) [25].

Fig. 7 (a) shows an experimental setup for through-wall imaging using an array of antennas. The setup has been used to detect a concealed object between two walls. Using the reflection coefficient (S11), a detection algorithm is applied to find the position of the object [72]. Fig. 7 (b) also demonstrates a scenario where people can be detected as objects on another side of the wall [52].
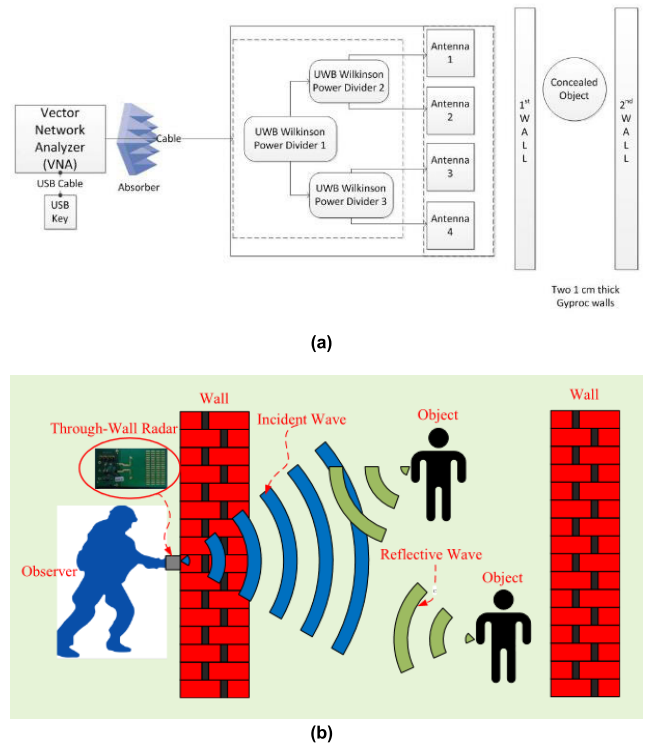

FIGURE 7. Configuration of a system for detecting a) concealed objects [72] b) humans behind a wall [52].

Another application similar to through-wall imaging is GPR. In the GPR system, electromagnetic waves are used to image materials underground. In the background, when an object has a different electrical characteristic from the ground, the scattered wave would have a different energy that can be used to detect the target [19], [20].

The GPR technology can be applied to a variety of materials and areas like archeology, desert soil inspection, boundary layer detection, airborne GPR, diffraction tomography, excavation, landmine detection, forensic surveys, real-time examination of pavements from moving vehicles, layered vegetation, wood and forest litter [18], [19], [20], [21]. Fig. 8 describes a GPR assessment of concrete conditions where the goal is to locate reinforcement bars.

GPR antenna design should take into account some specific factors. The antenna should have a wide frequency bandwidth to get a higher resolution. The radiation pattern, gain, and impedance matching of the antenna should all be consistent across the antenna's operational band. In addition, the majority of applications call for an antenna which is lightweight
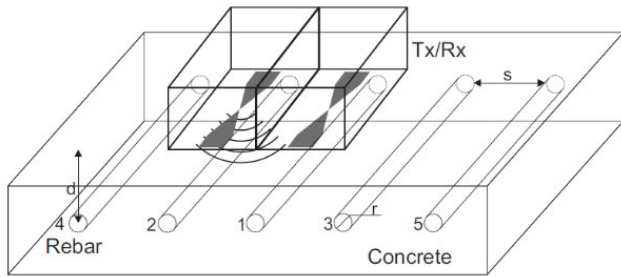
FIGURE 8. GPR assessment of concrete condition to find the location of reinforcement bars [19].

and compact in size. Specific physical qualities are needed to mount the device in small places [19].

A through-the-wall crowd counting (TWCC) system using Wi-Fi signals is also presented in [146]. The system is used to count the number of people who are working in an indoor environment. The system can be applied in hospitals, classrooms, stadiums, and other places where detecting personal activities is demanded. A phase ambiguity removal algorithm is presented in this paper, which results in almost 90 percent accuracy in recognition. Fig. 9 illustrates a general scheme of the TWCC system.
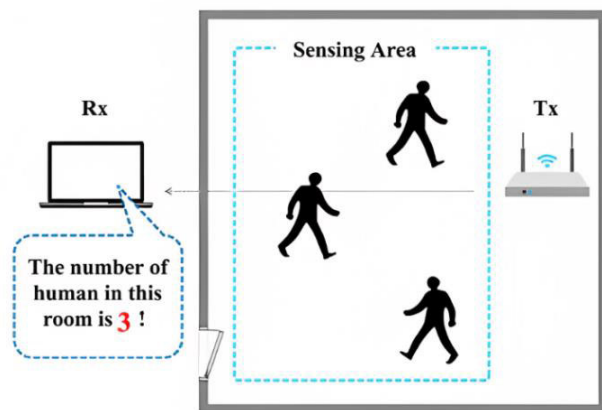
FIGURE 9. A schematic view of a TWCC system [146].

D. UWB SPECIFICATIONS BASED ON ITU
The operation bands, operational characteristics, and limitations for different UWB through-wall applications are summarized in Table 5. These specifications have been recommended by ITU in Rec. ITU-R SM.1756-0, and Rec. ITU-R SM.1755-0 [9], [147]. The recommended frequency for these applications is lower than 10.6 GHz, while the bandwidth can vary depending on the application.

IV. TECHNOLOGIES
A wide range of technologies is used for through-wall communications to enhance the transmitted wave behind a wall. Antennas are the main component of such an undertaking as

the main hubs of radiation through space. In addition, frequency selective surfaces, metasurfaces, and lenses are also utilized in through-wall applications. In this section, some papers which focus on these technologies for through-wall communications are reviewed.

A. ANTENNAS, ARRAYS, AND DIELECTRIC LENSES
Antennas for through-wall applications should have a high gain to guarantee transferring waves to another side of the wall. They should also have ultra-wide bandwidth to improve the resolution for imaging applications. The most popular antennas for through-wall applications are Vivaldi, horn, bow tie, and microstrip patch antennas.

Thanks to its medium gain and wideband properties, the Vivaldi antenna is widely used for through-wall imaging. Fig. 10 (a) shows a conventional Vivaldi antenna for this application. In order to improve the gain and bandwidth of these antennas, corrugations and grating elements have been added [54]. Fig. 10 (b) shows the schematic of the proposed antenna.
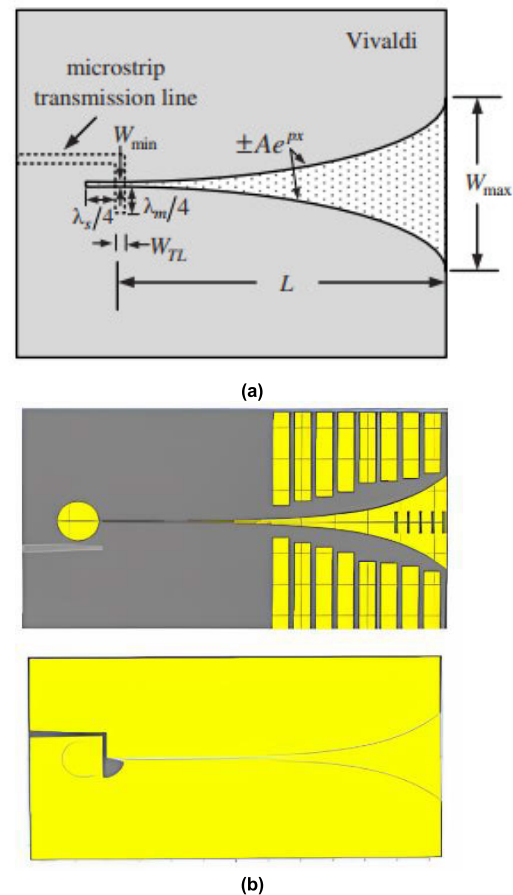

FIGURE 10. a) Conventional Vivaldi antenna [148] b) top and bottom view of the modified antenna [54].

The antenna has been designed on a low-cost FR-4 substrate. Using this structure, the gain of the antenna has increased to a maximum of 8.2 dBi, and the impedance

TABLE 5. Required specifications for different UWB through-wall applications [9], [147].

Application	Operation bands	Operational characteristics	Limitations of the service
GPR	The UWB bandwidth of an imaging system must be below 10.6 GHz	– Occasional use by professionals at infrequent intervals and specific sites – A specific application may have a limited number of devices that operate in continuous mobile use on roadways – Transmission is directed toward the ground	Operation is limited to purposes associated with law enforcement, firefighting, emergency rescue, scientific research, commercial mining, or construction
Through-wall imaging systems (1)	Through-wall imaging systems with a UWB bandwidth below 960 MHz	– Device is transportable – Used by trained personnel: typically, police, emergency teams, security and military – Occasional use at infrequent intervals – Deployed in limited numbers – Transmission is directed toward a wall – Devices may operate at some distance from the wall to maximize operational safety in case of hostile action	Operation is limited to through-wall imaging systems operated by law enforcement, emergency rescue or firefighting organizations that are under the authority of a local or state government
Through-wall imaging systems (2)	For equipment operating with a center frequency between 1.99 GHz and 10.6 GHz		This equipment may be operated only for law enforcement applications, providing emergency services, and necessary training operations
Indoor communication systems	The bandwidth of an indoor UWB system must be contained between 3.1 GHz and 10.6 GHz	– High-density use may occur in specific indoor environments such as office buildings – Some applications have occasional use, such as a UWB wireless mouse; others will operate at a higher percentage of the time, such as a video link – Outdoor use may also occur	Operation is limited to UWB transmitters employed solely for indoor operation

bandwidth reached 145.3 % at 6.95 GHz. The obtained results clearly show that this antenna is suitable for the frequency band of 1.9 to 12 GHz and through-wall radar applications.

A direct comparison between a double-ridge horn, the same antenna filled with sawdust, and a bow-tie antenna working at 0.5 to 1.5 GHz has been indicated in [56]. Fig. 11 (a) shows the tested antennas. Sawdust has been used to improve the impedance matching between the antenna and concrete in GPR applications. The measured results for three antenna gains are demonstrated in Fig.11 (b). In order to evaluate the matching between antennas and the background for GPR purposes, a slap of concrete with 10 cm thickness has been put between two identical antennas, and the S21 has been measured. Fig. 11 (c) shows the measured S21 for the three antennas. It can be seen that the horn antennas have a better performance in terms of energy in target, and the usage of sawdust can improve the performance of the horn antenna in lower frequencies.

In addition to well-known Vivaldi, horn, microstrip, and bow-tie antennas, other antennas can also be used for through-wall applications. In [63] a magneto-electric dipole antenna for ultra-wideband through-the-wall radar (UWB-TWR) application is provided and fabricated. This design aims to achieve a relative bandwidth of 66.67%' from 2.0 GHz to 4.0 GHz and a wide beam over the operating bandwidth. To obtain these specifications, a two-input one-output antenna array has been designed that enables the detection of the multi-targets behind the wall.

The antenna includes a vertically oriented quarter-wave shorted patch and a planar dipole, making the structure a mix of an electric dipole and a magnetic dipole. The antenna has been miniaturized by furrowing the radiating part of the electric dipole. Raising the horizontal beam width has also been obtained by tilting and bending the dipoles. To eliminate the backward radiation, a large ground plate has been utilized. Fig. 12 shows a photo of the fabricated antenna.

Antenna arrays have also been used to increase the gain for through-wall applications. In [72], an array of modified Vivaldi antennas has been fed using a modified Wilkinson power divider. Using a 4-element antenna array, a gain level in the range of about 15 dBi is achieved at the frequency range between 3.1 to 10.6 GHz. Fig. 13 (a) shows the antenna element and the power divider is illustrated in Fig. 13 (b). The antenna array has enabled an imaging system to detect concealed objects between two walls.

Furthermore, dielectric lenses can be used in connection with antennas to improve the directivity for through-wall communications. For instance, [110] presents a Vivaldi antenna in combination with a dielectric lens. The antenna contains a modified Vivaldi loaded with a dielectric lens. A Plexiglas frame is also employed to hold the dielectric lens. The structure of the antenna, including the dielectric lens and supporting frame, is shown in Fig. 14. The measured results show that the antenna with lens provides a gain level over 15 dBi with 160 percent fractional bandwidth, which covers the frequency range between 650 MHz and 6 GHz.

Table 6 presents a comparative analysis encompassing operational frequency, bandwidth, gain, substrate material, and dimensions of diverse antennas and arrays utilized for through-wall applications. Horn antennas and antennas employing dielectric lenses exhibit substantial gain and offer ultra-wideband (UWB) frequency bandwidth for through-wall communications. However, their drawback lies in their bulky form and limited integration compatibility with MMICs. On the other hand, array antennas featuring planar configurations offer both high gain and ample bandwidth for through-wall applications.
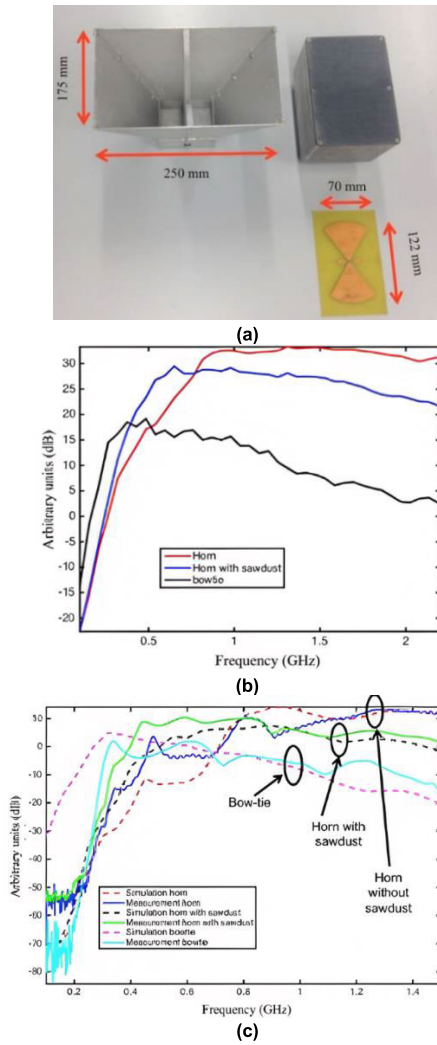
(a)

(b)

(c)

FIGURE 11. a) Tested antennas b) gain vs frequency of the horn, horn filled with sawdust and the bow tie antennas c) measured and simulated S21 for the three antennas [56].
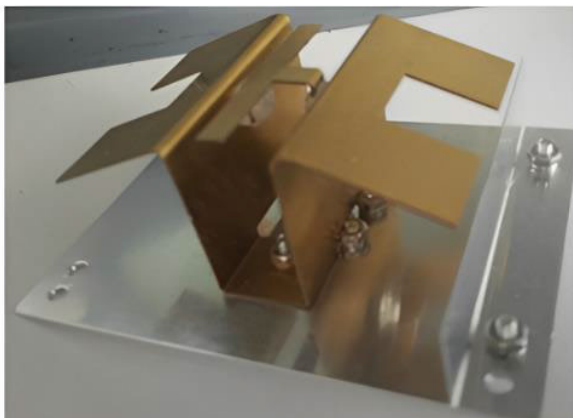

FIGURE 12. The fabricated Magneto-electric dipole antenna for through-wall applications [63].

The table also addresses the tunability aspect of these structures. Notably, the reported designs lack tunability tailored
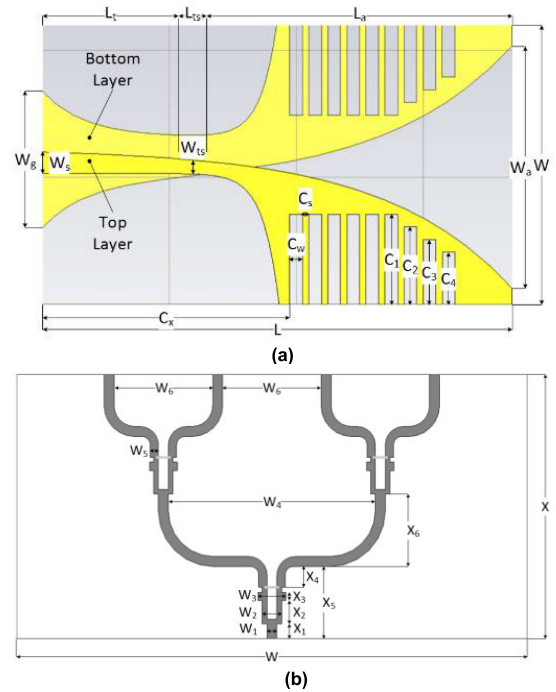

(a)

(b)

FIGURE 13. a) Antenna array element b) Wilkinson power divider [72].
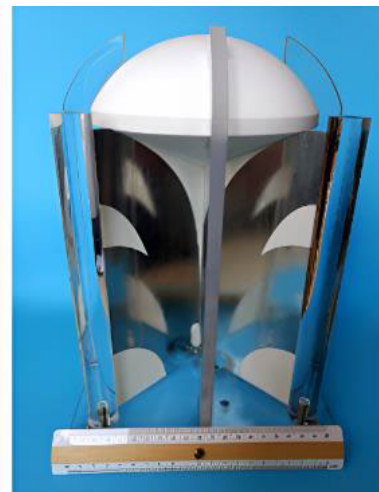
FIGURE 14. Vivaldi antenna with dielectric lens [110].

for through-wall applications, even though incorporating tunability could potentially enhance system performance. Antenna arrays equipped with reconfigurable beam patterns hold promise in imaging systems, enabling target tracking across various positions.

B. PERIODIC STRUCTURES

In recent years, periodic structures have been used in many applications to improve the performance of communications systems. FSSs, metasurface, and lenses have been employed in through-wall communications to improve the selectivity, matching, and penetration in these applications.

TABLE 6. A comparison between different non-tunable antennas used for through-wall communication.

Structure	Reference	ε_r	Center frequency (GHz)	Bandwidth (percent)	Maximum gain	Dimension (λ_0^3)
Vivaldi antenna	[54]	4.3	6.95	145.3	8.2	2.97×1.62×0.018
Horn antenna	[55]	metallic	1.4	UWB	21.5	10×6.25×3.17
Bow-tie antenna	[57]	2.55	1.55	96	4	0.84×0.33×0.008
Microstrip antenna	[59]	4.3	6.6	72.7	8	0.8×0.53×0.035
Antenna array	[72]	2.2	6.85	109.4	15	4.5×3.44×0.019
Dielectric loaded antenna	[110]	3.38 (antenna), 2.1 (lens)	3.3	160	15	3.76×2.44×1.96

Frequency-selective structures have been applied in many applications to improve frequency selectivity. These structures include unit cells that can be used in transmitting or reflecting modes depending on the applications. FSSs can be considered spatial filters which allow electromagnetic waves to be transmitted/reflected at specific frequency bands.

In [88] a symmetric cross dumbbell design unit cell is used to provide a reconfigurable FSS for RF shielding in an indoor wireless environment. The frequency response of this structure has angular stability up to 60 degrees. With rotation around the axis, different elements of the dumbbell shape FSS are excited, which results in three-band operation at 4.75, 3.2, and 5.2 GHz. Fig. 15 (a) shows the unit cell of this structure, and its measurement setup, including 15 × 11 elements, is illustrated in Fig. 15 (b). The measured transmission is 32 dB at 5.2 GHz, which demonstrates the level of blockage enforced by the FSS.

To gain the benefits of both antenna arrays and FSSs, a 2.4 GHz planar 2 × 2 array antenna combined with frequency selective surface is presented in [70]. A two-layer modified Jerusalem cross FSS, as shown in Fig.16 (a) and (d), is placed in front of the antenna array. Fig. 16 (b) and (c) demonstrate the modified 2 × 2 phased array antenna as the radiating element. The antenna array and additional FSS can obtain a gain of 13.1 dB and 70% efficiency, which operates at 2.4 GHz.

A dynamically reconfigurable metasurface antenna (DMA) for through-wall applications has been investigated in [91]. The structure includes a single-fed microstrip line which feeds metamaterial radiators. Metamaterial resonators are combined with diodes, which can be switched ON or OFF using an external voltage. Radiating and non-radiating modes can be achieved by turning switches ON and OFF, respectively. When an element is OFF, it does not perturb the energy passing through, which allows the wave to excite the subsequent elements. In an ON state, a portion of the power is radiated through space by the turned-on element. The superposition of the fields radiated by a collection of ON elements produces the radiation pattern of the
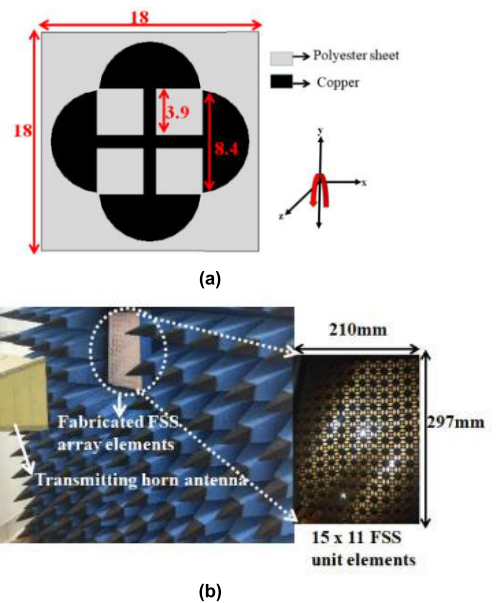
FIGURE 15. a) Cross dumbbell-shaped FSS unit cell b) measurement set up with 15 × 11 FSS unit elements [88].

overall DMA. This makes the structure tunable in the case of radiation patterns. The proposed antenna operates at K-band (18.8-26.5 GHz), and its application for through-wall imaging has been tested. Fig. 17 (a) and (b) demonstrate a schematic view of a microstrip-based dynamic metasurface antenna, including the unit cell.

Another alternative for improving the power of signal behind a wall is implementing lenses in through-wall communications systems. These lenses can be placed on the wall to improve the radiation properties. Fig. 18 illustrates a mechanism which enhances signal penetration through a wall by a metalens. In this scenario, the metalens is employed to increase the signal's power in indoor communications by focusing the electromagnetic waves on a Wi-Fi extender on the other side of the wall.
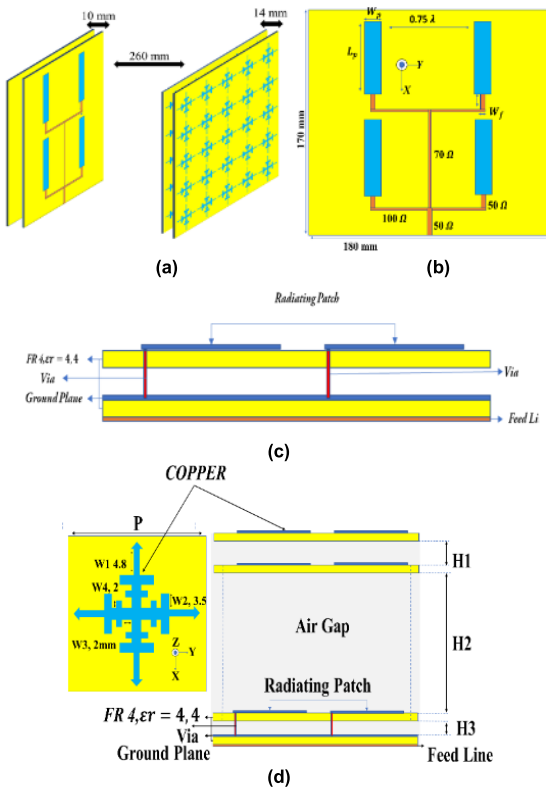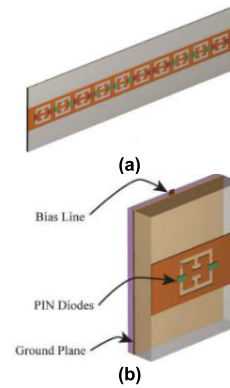
FIGURE 16. The structure of the antenna array in combination with FSS a) 3D view b) antenna array with feeding network c) the geometry of double layer antenna array d) combination of the antenna array and FSS [70].

FIGURE 17. Metasurface antenna for through-wall imaging applications a) structure of the microstrip-based dynamic antenna b) 3D view of the unit cell [91].

FIGURE 18. Improving the power of the signal behind a wall using metalens [109].

In [109], a multilayer ultrathin metalens has been introduced to focus the electromagnetic wave to the other side of the wall. The metalens unit cells are illustrated in Fig. 19 (a) and (b). The effect of unit cell width (w) and the radius of the metal via (r) on the transfer index for two types of metaatoms at 5 GHz are also demonstrated in this figure.
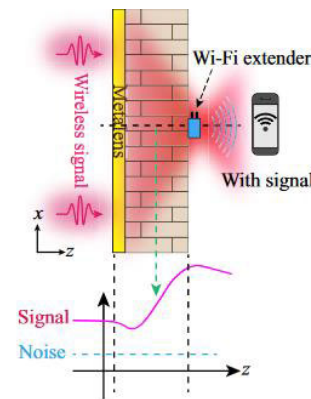
Each unit cell consists of three layers of metallic patterns. The meta-atoms unit cell can provide a high transmission amplitude of about 85 percent on average. The combination of two meta-atoms can also provide about 2π phase shifts, which are required for the design of metalenses. The final 20×20 designed metalens is shown in Fig. 19 (c).

To validate the structure, it has been used in a 5-GHz Wi-Fi system. The measurement setup is shown in Fig. 20 (a). Fig. 20 (b) illustrates the results of download and upload speed, signal power, and latency versus transmitted power. It is obvious that metalens has improved the reliability of the communication link on the other side of the wall.

The primary attributes of periodic structures used for through-wall applications, such as center frequency, substrate dielectric constant, operational bandwidth, dimensions, and tunability, are presented in Table 7. Periodic structures can be used in combination with antennas to enhance radiation performance and introduce tunability to the system. Achieving tunability in these structures can be realized through mechanisms like pin diodes or mechanical adjustments.

In comparison to antennas, periodic structures may exhibit bulkier dimensions. Furthermore, they are typically fixed once employed. While this aspect poses no challenges in indoor applications, it might prove impractical in imaging systems. Conversely, compact Frequency Selective Surfaces in conjunction with antennas offer the advantages of reduced profile and can find utility across various applications.

V. PROSPECTS

Some possible research areas have been listed in this section that can be considered by researchers for future studies.

A. TUNABILITY AND ADAPTIVELY

Depending on the application, through-wall technologies can be maintained in different environments. In some applications, the accuracy of the results can be affected by temperature or other environmental variations. For instance, the material's thickness and dielectric constant vary in different applications. Therefore, it would be important to make these technologies tunable for adapting them to new situations.

In through-wall imaging, the goal of the system is to detect an object or human behind an obstacle. In most of the

TABLE 7. A comparison between different periodic structures used for through-wall communication.

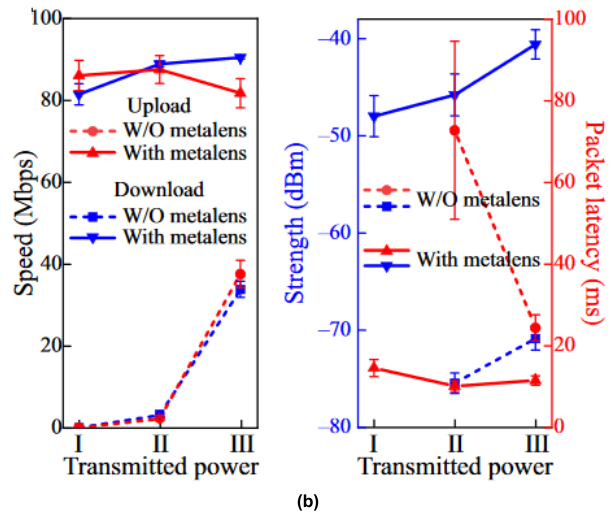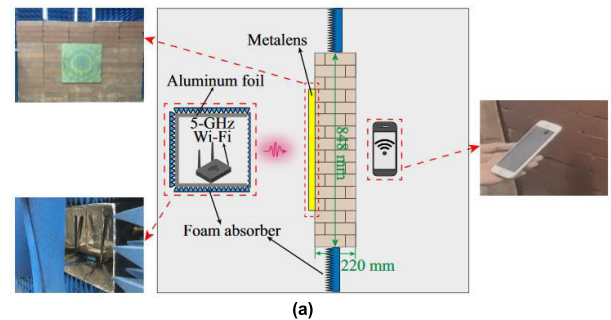| Structure	Reference	ε_r	Center frequency (GHz)	Bandwidth (percent)	Dimension (λ_0^3)	Tunability/ mechanism
Metasurface	[91]	-	22.65	34	-	Yes/ Pin diodes
FSS	[88]	2.8	3.2 to 5.5	~ 16	5.21×3.68×0.001	Yes/ mechanically
FSS/Array	[70]	4.4	2.4	-	1.44×1.36×0.112	no
Metalens	[109]	4.3	5	24	6.3×6.3×0.1	no
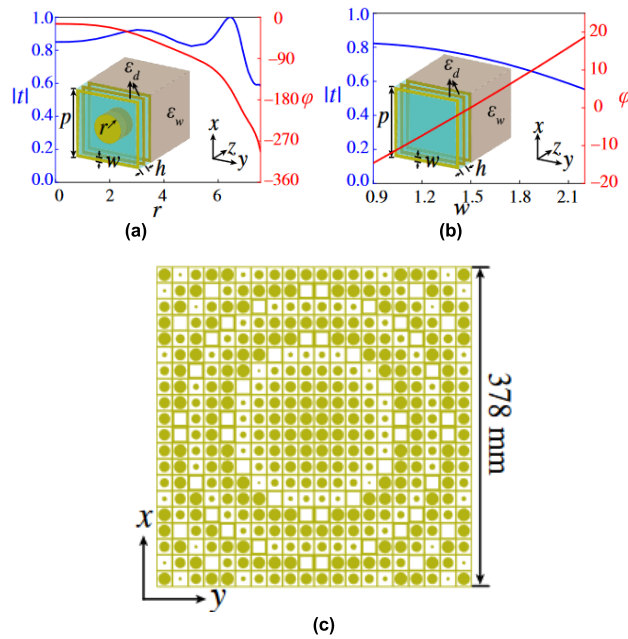
FIGURE 19. a) Metalens unit cell and the results of simulated transmission amplitudes (blue), and phase (red) as a function of the via radius (r) b) the variation of the transmission amplitude and phase as a function of w for the metalens without via c) the structure of a 20 × 20 metaatoms lens [109].

FIGURE 20. a) Experimental setup b) the measured results for download and upload speed, signal power and latency with and without metalens. Error bars are presented to show the measurement error for repeated tests [109].

experimental setups, walls are concrete or bricks. However, in real situations, an imaging system should work in different environments with different materials used in the wall. The system should have the ability to adapt itself to these materials. A realistic situation would be the application of the system in an earthquake crisis. There would be many rubbles in the background, and the system should have the ability to change its parameters based on the materials in order to increase the accuracy of the results.

Moreover, to the best of our knowledge, there is little work on the effect of polarization in penetrating waves through different walls. A polarization switchable technology using antennas or FSSs can be mentioned for through-wall applications. In some walls, linear polarization might have better penetration, while in others, circular or elliptical polarization might be useful.

In addition, as mentioned in Section III and summarized in Table 5, different applications of through-wall communications can work in different frequency bands with different bandwidths. Designing a system which can change the operating frequency or bandwidth can provide a structure to be applied in different scenarios.

B. APPLICATION OF 3D PRINTING TECHNOLOGY

In recent years, the application of 3D printers in the fabrication process of many components has increased thanks to their low cost and fast implementation process [149], [150]. It has been previously used in the design of antennas [150], [151], [152], [153], [154] and other microwave components [149], [155], [156].
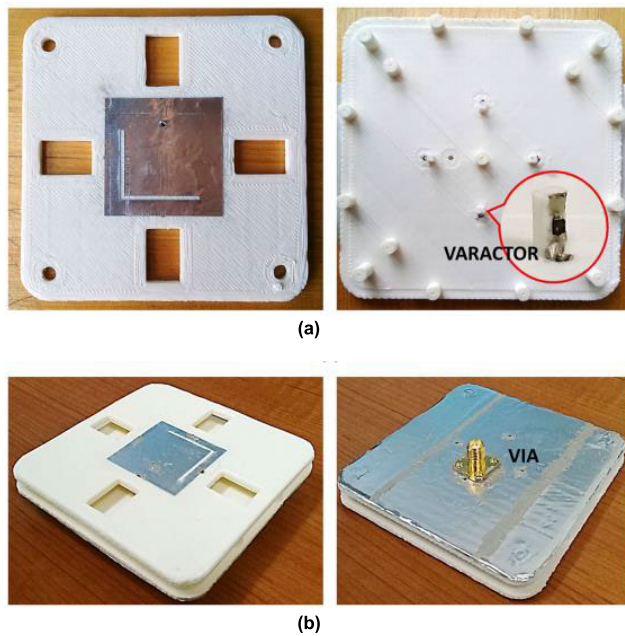
FIGURE 21. An antenna fabricated using 3D printing process a) Top view of the antenna including the patch (right). The bottom layer includes varactors (shown inset) with supported cylindrical posts (left). (b) the complete fabricated antenna [152].

Implementation of through-wall technologies with the 3D printing process can reduce fabrication costs and improve the accuracy of the design. In addition, these printers can be used to fabricate complex geometries that cannot be built with the traditional process.

Furthermore, some new materials which would be hard to fabricate using traditional techniques can be easily used in the 3D process. These materials, including graphene, liquid crystal, and barium strontium titanate (BST), can be employed to make the structures tunable and adaptive for different applications.

For instance, Fig. 21 shows a tunable circularly polarized patch antenna which has been fabricated using 3D printing technology [152]. The antenna has been implemented using two layers of acrylonitrile butadiene styrene (ABS) with air in between. The 3D printing process has enabled the designer to add varactors between the patch and ground vertically, which resulted in the lower parasite.

VI. CONCLUSION

The article presents a comprehensive review on through-wall communications, including wall characterization, technologies, and applications, with examples provided in each section. Antennas, frequency selective surfaces, metasurfaces, and lenses were discussed as common technologies used in through-wall communications.

The most typical application of through-wall communication is indoor communication, where electromagnetic waves propagate through walls and other dielectric materials. Other popular research topics in this area include imaging through walls for object and human detection, human counting, and ground penetration radar to detect objects underground. Another branch of through-wall communication is power transfer through dielectric walls, which has gained more attention in recent years, including energy harvesting.

The paper also highlighted the potential of 3D printing for the fabrication of antennas and other technologies due to its ability to realize complex geometries and employ new materials in the process.

For future research, the article recommended tunable technologies that use tunable material to enable real-time variation of the system. Additionally, such technologies have the potential of realizing adaptation to new environments and materials and can be the subject of further studies as such.

REFERENCES

[1] S. Helhel, "Comparison of 900 and 1800 MHz indoor propagation deterioration," *IEEE Trans. Antennas Propag.*, vol. 54, no. 12, pp. 3921–3924, Dec. 2006, doi: 10.1109/TAP.2006.884311.

[2] D. Zeng, G. Lu, and J. Lin, "Measurement at 820 MHz for indoor wave propagation," in *Proc. 5th Asia–Pacific Conf. Environ. Electromagn.*, Sep. 2009, pp. 204–207, doi: 10.1109/CEEM.2009.5305710.

[3] G. Narimani, P. A. Martin, and D. P. Taylor, "Analysis of ultrawideband pulse distortion due to lossy dielectric walls and indoor channel models," *IEEE Trans. Antennas Propag.*, vol. 64, no. 10, pp. 4423–4433, Oct. 2016, doi: 10.1109/TAP.2016.2593875.

[4] Y. Wang, H. Zheng, and X. Chu, "Impact of wall blockage on LOS user association strategy in indoor small cell networks," in *Proc. Int. Symp. Antennas Propag. (ISAP)*, Jan. 2021, pp. 579–580, doi: 10.23919/ISAP47053.2021.9391246.

[5] Z. Li, H. Hu, J. Zhang, and J. Zhang, "Impact of wall penetration loss on indoor wireless networks," *IEEE Antennas Wireless Propag. Lett.*, vol. 20, no. 10, pp. 1888–1892, Oct. 2021, doi: 10.1109/LAWP.2021.3099339.

[6] K. Sayidmarie, A. H. Aboud, and M. S. Salim, "Estimation of wall penetration loss for indoor WLAN systems," in *Proc. 6th Int. Conf. Sci. Electron., Technol. Inf. Telecommun. (SETIT)*, Mar. 2012, pp. 675–679, doi: 10.1109/SETIT.2012.6481994.

[7] L. Nagy, "Short range device (SRD) propagation modeling for indoor environment," in *Proc. 16th IST Mobile Wireless Commun. Summit*, Jul. 2007, pp. 1–5.

[8] Z. Zhao, L. Kong, Y. Jia, and J. Liu, "An estimation approach for equivalent wall parameters in through-wall-radar imaging," in *Proc. IET Int. Radar Conf.*, Apr. 2013, pp. 1–4.

[9] *Framework for the Introduction of Devices Using Ultra-Wideband Technology*, document ITU_R 1756, 2023.

[10] *IEEE Standard for Safety Levels With Respect to Human Exposure to Electric, Magnetic, and Electromagnetic Fields, 0 Hz to 300 GHz*, Standard C95.1-2019, Institute of Electrical and Electronics Engineers, New York, NY, USA, 2019.

[11] International Commission on Non-Ionizing Radiation Protection, "Guidelines for limiting exposure to Electromagnetic Fields (100 kHz to 300 GHz)," *Health Phys.*, vol. 118, no. 5, pp. 483–524, May 2020.

[12] N. Qasem and R. Seager, "Environmental modification to enhance indoor wireless communication system," in *Proc. Loughborough Antennas Propag. Conf. (LAPC)*, Nov. 2012, pp. 1–4, doi: 10.1109/LAPC.2012.6402982.

[13] M. Gustafsson, A. Karlsson, A. P. P. Rebelo, and B. Widenberg, "Design of frequency selective windows for improved indoor outdoor communication," *IEEE Trans. Antennas Propag.*, vol. 54, no. 6, pp. 1897–1900, Jun. 2006, doi: 10.1109/TAP.2006.875926.

[14] N. Qasem and R. Seager, "Frequency selective wall for enhancing wireless signal in indoor environments," in *Proc. Loughborough Antennas Propag. Conf.*, Nov. 2009, pp. 573–576, doi: 10.1109/LAPC.2009.5352395.

[15] L. Subrt, P. Pechac, L. Ford, R. Langley, and J. Rigelsford, "Controlling coverage for indoor wireless networks using metalized active FSS walls," in *Proc. 19th Asia–Pacific Conf. Commun. (APCC)*, Aug. 2013, pp. 496–500, doi: 10.1109/APCC.2013.6765998.

[16] G. Sung, K. Sowerby, M. Neve, and A. Williamson, "A frequency-selective wall for interference reduction in wireless indoor environments," *IEEE Antennas Propag. Mag.*, vol. 48, no. 5, pp. 29–37, Oct. 2006, doi: 10.1109/map.2006.277152.

[17] Y. Zhang, C. Chen, S. Yang, J. Zhang, X. Chu, and J. Zhang, "How friendly are building materials as reflectors to indoor LOS MIMO communications," *IEEE Internet Things J.*, vol. 7, no. 9, pp. 9116–9127, Sep. 2020, doi: 10.1109/JIOT.2020.3004008.

[18] M. J. Oyan, S.-E. Hamran, L. Hanssen, T. Berger, and D. Plettemeier, "Ultrawideband gated step frequency ground-penetrating radar," *IEEE Trans. Geosci. Remote Sens.*, vol. 50, no. 1, pp. 212–220, Jan. 2012, doi: 10.1109/TGRS.2011.2160069.

[19] X. L. Travassos, S. L. Avila, R. L. D. S. Adriano, and N. Ida, "A review of ground penetrating radar antenna design and optimization," *J. Microw., Optoelectron. Electromagn. Appl.*, vol. 17, no. 3, pp. 385–402, Sep. 2018, doi: 10.1590/2179-10742018v17i31321.

[20] H. Liu, H. Lu, J. Lin, F. Han, C. Liu, J. Cui, and B. F. Spencer, "Penetration properties of ground penetrating radar waves through rebar grids," *IEEE Geosci. Remote Sens. Lett.*, vol. 18, no. 7, pp. 1199–1203, Jul. 2021, doi: 10.1109/LGRS.2020.2995670.

[21] M. Pieraccini, "Noise performance comparison between continuous wave and stroboscopic pulse ground penetrating radar," *IEEE Geosci. Remote Sens. Lett.*, vol. 15, no. 2, pp. 222–226, Feb. 2018, doi: 10.1109/LGRS.2017.2781458.

[22] Z. Tahar, X. Derobert, and M. Benslama, "An ultra-wideband modified Vivaldi antenna applied to through the ground and wall imaging," *Prog. Electromagn. Res. C*, vol. 86, pp. 111–122, 2018.

[23] H. Li, G. Cui, L. Kong, S. Guo, and M. Wang, "Scale-adaptive human target tracking for through-wall imaging radar," *IEEE Geosci. Remote Sens. Lett.*, vol. 17, no. 8, pp. 1348–1352, Aug. 2020, doi: 10.1109/LGRS.2019.2948629.

[24] T. V. Hoang, R. Kumar, T. Fromenteze, M. García-Fernández, G. Álvarez-Narciandi, V. Fusco, and O. Yurduseven, "Frequency selective computational through wall imaging using a dynamically reconfigurable metasurface aperture," *IEEE Open J. Antennas Propag.*, vol. 3, pp. 353–362, 2022, doi: 10.1109/OJAP.2022.3161128.

[25] K. Raha and K. P. Ray, "Through wall imaging radar antenna with a focus on opening new research avenues," *Defence Sci. J.*, vol. 71, no. 5, pp. 670–681, Sep. 2021, doi: 10.14429/dsj.71.16592.

[26] Y.-C. Li, D. Oh, S. Kim, and J.-W. Chong, "Dual channel S-band frequency modulated continuous wave through-wall radar imaging," *Sensors*, vol. 18, no. 2, p. 311, Jan. 2018, doi: 10.3390/s18010311.

[27] H.-n. Wang, B.-y. Lu, Z.-m. Zhou, and Q. Song, "Through-the-wall imaging and correction based on the estimation of wall parameters," in *Proc. IEEE CIE Int. Conf. Radar*, vol. 2, Oct. 2011, pp. 1327–1330, doi: 10.1109/CIE-Radar.2011.6159802.

[28] H. Alidoustaghdam, S. Dogu, M. N. Akinci, and M. Çayören, "Through-the-wall microwave imaging with minimum antennas and an auxiliary metallic bar," in *Proc. IEEE Asia–Pacific Microw. Conf. (APMC)*, Dec. 2020, pp. 1054–1056, doi: 10.1109/APMC47863.2020.9331597.

[29] Z. Hu, Z. Zeng, K. Wang, W. Feng, J. Zhang, Q. Lu, and X. Kang, "Design and analysis of a UWB MIMO radar system with miniaturized Vivaldi antenna for through-wall imaging," *Remote Sens.*, vol. 11, no. 16, p. 1867, Aug. 2019, doi: 10.3390/rs11161867.

[30] M. G. Amin, *Through-the-Wall Radar Imaging*. Boca Raton, FL, USA: CRC Press, 2017.

[31] P. K. M. Nkwari, S. Sinha, and H. C. Ferreira, "Through-the-wall radar imaging: A review," *IETE Tech. Rev.*, vol. 35, pp. 631–639, Oct. 2018.

[32] B. Yektakhah and K. Sarabandi, "All-directions through-the-wall imaging using a small number of moving omnidirectional bi-static FMCW transceivers," *IEEE Trans. Geosci. Remote Sens.*, vol. 57, no. 5, pp. 2618–2627, May 2019.

[33] K. Sun, Y. Wu, F. Qian, H. Jung, S. Kaluvan, H. Huijin, C. Zhang, F. K. Reed, M. Nance Ericson, H. Zhang, and L. Zuo, "Self-powered through-wall communication for dry cask storage monitoring," *Ann. Nucl. Energy*, vol. 177, Nov. 2022, Art. no. 109306, doi: 10.1016/j.anucene.2022.109306.

[34] L. Huang, A. P. Hu, A. Swain, S. Kim, and Y. Ren, "An overview of capacitively coupled power transfer—A new contactless power transfer solution," in *Proc. IEEE 8th Conf. Ind. Electron. Appl. (ICIEA)*, Jun. 2013, pp. 461–465, doi: 10.1109/ICIEA.2013.6566413.

[35] X. Gao, H. R. Sadjadpour, F. U. Dowla, and F. Nekoogar, "Through-wall UWB communications with limited transmit power," in *Proc. 11th Electr. Power, Electron., Commun., Controls Informat. Seminar (EECCIS)*, Aug. 2022, pp. 170–175, doi: 10.1109/EECCIS54468.2022.9902902.

[36] Y.-S. Seo, Z. Hughes, M. Hoang, D. Isom, M. Nguyen, S. Rao, and J.-C. Chiao, "Investigation of wireless power transfer in through-wall applications," in *Proc. Asia–Pacific Microw. Conf.*, Dec. 2012, pp. 403–405, doi: 10.1109/APMC.2012.6421612.

[37] D.-X. Yang, Z. Hu, H. Zhao, H.-F. Hu, Y.-Z. Sun, and B.-J. Hou, "Through-metal-wall power delivery and data transmission for enclosed sensors: A review," *Sensors*, vol. 15, no. 12, pp. 31581–31605, Dec. 2015, doi: 10.3390/s151229870.

[38] A. K. RamRakhyani, S. Mirbabasi, and M. Chiao, "Design and optimization of resonance-based efficient wireless power delivery systems for biomedical implants," *IEEE Trans. Biomed. Circuits Syst.*, vol. 5, no. 1, pp. 48–63, Feb. 2011, doi: 10.1109/TBCAS.2010.2072782.

[39] D. A. Shoudy, G. J. Saulnier, H. A. Scarton, P. K. Das, S. Roa-Prada, J. D. Ashdown, and A. J. Gavens, "P3F-5 an ultrasonic through-wall communication system with power harvesting," in *Proc. IEEE Ultrason. Symp.*, Oct. 2007, pp. 1848–1853.

[40] M. K. Müller, M. Taranetz, and M. Rupp, "Analyzing wireless indoor communications by blockage models," *IEEE Access*, vol. 5, pp. 2172–2186, 2017.

[41] S. Bakirtzis, J. Chen, K. Qiu, J. Zhang, and I. Wassell, "EM DeepRay: An expedient, generalizable, and realistic data-driven indoor propagation model," *IEEE Trans. Antennas Propag.*, vol. 70, no. 6, pp. 4140–4154, Jun. 2022.

[42] I.-J. Yoon and H. Ling, "Investigation of near-field wireless power transfer in the presence of lossy dielectric materials," *IEEE Trans. Antennas Propag.*, vol. 61, no. 1, pp. 482–488, Jan. 2013, doi: 10.1109/TAP.2012.2215296.

[43] M. Škiljo and Z. Blažević, "Interaction between humans and wireless power transfer systems," in *Proc. 22nd Int. Conf. Softw., Telecommun. Comput. Netw. (SoftCOM)*, Sep. 2014, pp. 15–18, doi: 10.1109/SOFTCOM.2014.7039101.

[44] S. Y. R. Hui, W. Zhong, and C. K. Lee, "A critical review of recent progress in mid-range wireless power transfer," *IEEE Trans. Power Electron.*, vol. 29, no. 9, pp. 4500–4511, Sep. 2014, doi: 10.1109/TPEL.2013.2249670.

[45] X. Shi, C. Qi, and S. Ye, "Effects of obstacle sizes on wireless power transfer via magnetic resonance coupling," in *Proc. IEEE PELS Workshop Emerg. Technolog., Wireless Power (WoW)*. Union City, NJ, USA: Wire, Jun. 2015, pp. 1–5, doi: 10.1109/WoW.2015.7132833.

[46] C. Rong, C. Lu, Y. Zeng, X. Tao, X. Liu, R. Liu, X. He, and M. Liu, "A critical review of metamaterial in wireless power transfer system," *IET Power Electron.*, vol. 14, no. 9, pp. 1541–1559, Jul. 2021, doi: 10.1049/pel2.12099.

[47] J. C. Olivares-Galvan, E. Campero-Littlewood, S. Maximov, S. Magdaleno-Adame, and W. Xu, "Wireless power transfer: Literature survey," in *Proc. IEEE Int. Autumn Meeting Power Electron. Comput. (ROPEC)*, Nov. 2013, pp. 1–7, doi: 10.1109/ROPEC.2013.6702725.

[48] C. Liu, A. P. Hu, and N.-K. C. Nair, "Coupling study of a rotary capacitive power transfer system," in *Proc. IEEE Int. Conf. Ind. Technol.*, Feb. 2009, pp. 1–6, doi: 10.1109/ICIT.2009.4939623.

[49] S. V. Georgakopoulos and O. Jonah, "Optimized wireless power transfer to RFID sensors via magnetic resonance," in *Proc. IEEE Int. Symp. Antennas Propag. (APSURSI)*, Jul. 2011, pp. 1421–1424, doi: 10.1109/APS.2011.5996559.

[50] R. Cicchetti, S. Pisa, E. Piuzzi, E. Pittella, P. D'Atanasio, and O. Testa, "Numerical and experimental comparison among a new hybrid FT-music technique and existing algorithms for through-the-wall radar imaging," *IEEE Trans. Microw. Theory Techn.*, vol. 69, no. 7, pp. 3372–3387, Jul. 2021, doi: 10.1109/TMTT.2021.3061500.

[51] P. Nijhawan, A. Kumar, and Y. Dwivedi, "A flexible corrugated Vivaldi antenna for radar and see-through wall applications," in *Proc. 3rd Int. Conf. Microw. Photon. (ICMAP)*, Feb. 2018, pp. 1–2, doi: 10.1109/ICMAP.2018.8354628.

[52] J. Zhang, H. Lan, M. Liu, and Y. Yang, "A handheld nano through-wall radar locating with the gain-enhanced Vivaldi antenna," *IEEE Sensors J.*, vol. 20, no. 8, pp. 4420–4429, Apr. 2020, doi: 10.1109/JSEN.2019.2963234.

[53] F. Fioranelli, S. Salous, I. Ndip, and X. Raimundo, "Through-the-wall detection with gated FMCW signals using optimized patch-like and Vivaldi antennas," *IEEE Trans. Antennas Propag.*, vol. 63, no. 3, pp. 1106–1117, Mar. 2015, doi: 10.1109/TAP.2015.2389793.

[54] A. Kuriakose, T. A. George, and S. Anand, "Improved high gain Vivaldi antenna design for through-wall radar applications," in *Proc. Int. Symp. Antennas Propag. (APSYM)*, Dec. 2020, pp. 58–61.

[55] A. Karanth, N. Onkar, N. S. N. Smitha, Sridhara, and V. Singh, "Through-wall imaging system using horn antennas," in *Proc. 4th Int. Conf. Adv. Comput. Commun. Syst. (ICACCS)*, Jan. 2017, pp. 1–6.

[56] M. Pieraccini, L. Miccinesi, and N. Rojhani, "Comparison between horn and bow-tie antennas for through-the-wall applications," in *Proc. IEEE Conf. Antenna Meas. Appl. (CAMA)*, Sweden, 2018, pp. 1–4, doi: 10.1109/CAMA.2018.8530531.

[57] Q. Lu, L. Zhou, C. Tan, and L. Guanghua, "A novel wide beam UWB antenna design for Through-the-Wall radar," in *Proc. Int. Conf. Microw. Millim. Wave Technol.*, May 2010, pp. 1912–1915, doi: 10.1109/ICMMT.2010.5524899.

[58] T. Hariyadi, A. Munir, A. Bayu Suksmono, K. Adi, and A. D. Setiawan, "Unidirectional broadband microstrip antenna for through walls radar application," in *Proc. Int. Conf. Electr. Eng. Informat.*, Jul. 2011, pp. 1–4, doi: 10.1109/ICEEI.2011.6021748.

[59] T. Hariyadi, Y. T. Huda, and B. Mulyanti, "A small ultra-wideband unidirectional microstrip antenna for through-wall radar application," *J. Telecommun., Electron. Comput. Eng. (JTEC)*, vol. 8, no. 1, pp. 25–28, 2016.

[60] F. Fioranelli, S. Salous, and I. Ndip, "Optmized patch-like antennas for through the wall radar imaging and preliminary results with frequency modulated interrupted continuous wave," in *Proc. Int. Symp. Signals, Syst., Electron. (ISSSE)*, Oct. 2012, pp. 1–5, doi: 10.1109/ISSSE.2012.6374334.

[61] D. Pinchera, M. D. Migliore, and F. Schettino, "An ultra wide permittivity antenna (UWPA) for reliable through-wall communications," *IEEE Trans. Antennas Propag.*, vol. 61, no. 2, pp. 957–960, Feb. 2013, doi: 10.1109/TAP.2012.2223439.

[62] J. Li, A. Zhang, J. Liu, and Q. H. Liu, "Cavity-backed wideband magneto-electric antenna for through-the-wall imaging radar applications," in *Proc. IEEE Radar Conf. (RadarConf)*, May 2016, pp. 1–3, doi: 10.1109/RADAR.2016.7485327.

[63] X. Zhao, G. Yan, T. Chang, C. H. Liang, Z. Wang, and H. Fu, "Antenna design for ultra-wideband through wall radar," in *Proc. 3rd IEEE Int. Conf. Comput. Commun. (ICCC)*, Dec. 2017, pp. 1121–1124, doi: 10.1109/CompComm.2017.8322718.

[64] J. Shao, G. Fang, Y. Ji, K. Tan, and H. Yin, "A novel compact tapered-slot antenna for GPR applications," *IEEE Antennas Wireless Propag. Lett.*, vol. 12, pp. 972–975, 2013.

[65] F. Zhang, G.-Y. Fang, Y.-C. Ji, H.-J. Ju, and J.-J. Shao, "A novel compact double exponentially tapered slot antenna (DETSA) for GPR applications," *IEEE Antennas Wireless Propag. Lett.*, vol. 10, pp. 195–198, 2011.

[66] J. Ali, N. Abdullah, M. Yusof, E. Mohd, and S. Mohd, "Ultra-wideband antenna design for GPR applications: A review," *Int. J. Adv. Comput. Sci. Appl.*, vol. 8, no. 7, pp. 1–9, 2017.

[67] H. R. Heidari, P. Rezaei, S. Kiani, and M. Taherinezhad, "A monopulse array antenna based on SIW with circular polarization for using in tracking systems," *AEU Int. J. Electron. Commun.*, vol. 162, Apr. 2023, Art. no. 154563.

[68] F. Sakai, A. Suzuki, O. Kazuo, M. Makimoto, and K. Sawaya, "A UWB through-wall radar using beam scanning array antenna," in *IEEE MTT-S Int. Microw. Symp. Dig.*, Jun. 2011, pp. 1–4, doi: 10.1109/MWSYM.2011.5972774.

[69] Y.-J. Ren, C.-P. Lai, P.-H. Chen, and R. M. Narayanan, "Compact ultrawideband UHF array antenna for through-wall radar applications," *IEEE Antennas Wireless Propag. Lett.*, vol. 8, pp. 1302–1305, 2009, doi: 10.1109/LAWP.2009.2037985.

[70] R. A. I. Asyari, R. El Arif, W.-C. Su, and T.-S. Horng, "High gain array antenna with FSS for vital sign monitoring through the wall," 2022, arXiv:2203.12682.

[71] A. Rittiplang and P. Phasukkit, "1-Tx/5-Rx through-wall UWB switched-antenna-array radar for detecting stationary humans," *Sensors*, vol. 20, no. 23, p. 6828, Nov. 2020, doi: 10.3390/s20236828.

[72] A. Elboushi, D. Joanes, M. Derbas, S. Khaled, A. Zafar, S. Attabibi, and A. R. Sebak, "Design of UWB antenna array for through-wall detection system," in *Proc. IEEE Symp. Wireless Technol. Appl. (ISWTA)*, Sep. 2013, pp. 349–354, doi: 10.1109/ISWTA.2013.6688802.

[73] A. R. Buzdar, A. Buzdar, H. B. Tila, L. Sun, M. Khan, U. Khan, and W. Ferozv, "Low cost Vivaldi array antenna for mobile through wall sensing platforms," in *IEEE MTT-S Int. Microw. Symp. Dig.*, Mar. 2016, pp. 1–4, doi: 10.1109/IEEE-IWS.2016.7585487.

[74] N. V. Venkatarayalu and Y.-B. Gan, "Design of a tapered slot array antenna for UWB through-wall RADAR," in *Proc. IEEE Antennas Propag. Soc. Int. Symp.*, Jul. 2010, pp. 1–4, doi: 10.1109/APS.2010.5561131.

[75] M. Saikia and K. V. Srivastava, "A time modulated polarization rotating frequency selective surface," *IEEE Transactions Antennas Propag.*, vol. 71, no. 2, pp. 1506–1515, Feb. 2023, doi: 10.1109/TAP.2022.3217979.

[76] M. Hussein, J. Zhou, Y. Huang, and B. Al-Juboori, "A low-profile miniaturized second-order bandpass frequency selective surface," *IEEE Antennas Wireless Propag. Lett.*, vol. 16, pp. 2791–2794, 2017, doi: 10.1109/LAWP.2017.2746266.

[77] M. Kartal, J. J. Golezani, and B. Doken, "A triple band frequency selective surface design for GSM systems by utilizing a novel synthetic resonator," *IEEE Trans. Antennas Propag.*, vol. 65, no. 5, pp. 2724–2727, May 2017, doi: 10.1109/TAP.2017.2670230.

[78] P. M. Njogu, B. Sanz-Izquierdo, and E. A. Parker, "A liquid sensor based on frequency selective surfaces," *IEEE Trans. Antennas Propag.*, vol. 71, no. 1, pp. 631–638, Jan. 2023, doi: 10.1109/TAP.2022.3219540.

[79] M. Saikia, S. Ghosh, and K. V. Srivastava, "Design and analysis of ultrathin polarization rotating frequency selective surface using V-shaped slots," *IEEE Antennas Wireless Propag. Lett.*, vol. 16, pp. 2022–2025, 2017, doi: 10.1109/LAWP.2017.2693685.

[80] W. Yin, H. Zhang, T. Zhong, and X. Min, "Ultra-miniaturized low-profile angularly-stable frequency selective surface design," *IEEE Trans. Electromagn. Compat.*, vol. 61, no. 4, pp. 1234–1238, Aug. 2019, doi: 10.1109/TEMC.2018.2881161.

[81] R. Anwar, L. Mao, and H. Ning, "Frequency selective surfaces: A review," *Appl. Sci.*, vol. 8, no. 9, p. 1689, Sep. 2018, doi: 10.3390/app8091689.

[82] Z. Sun, L. Yan, X. Zhao, and R. X. Gao, "An ultrawideband frequency selective surface absorber with high polarization-independent angular stability," *IEEE Antennas Wireless Propag. Lett.*, vol. 22, no. 4, pp. 789–793, Apr. 2023, doi: 10.1109/LAWP.2022.3225582.

[83] M. Bashiri, C. Ghobadi, J. Nourinia, and M. Majidzadeh, "WiMAX, WLAN, and X-band filtering mechanism: Simple-structured triple-band frequency selective surface," *IEEE Antennas Wireless Propag. Lett.*, vol. 16, pp. 3245–3248, Nov. 2017, doi: 10.1109/LAWP.2017.2771265.

[84] P. Njogu, A. Shastri, S. Gao, and B. Sanz-Izquierdo, "Screen-printed FSS plasterboard for wireless indoor applications," in *Proc. Microw. Medit. Symp. (MMS)*, May 2022, pp. 1–4, doi: 10.1109/MMS55062.2022.9825506.

[85] U. Farooq, M. F. Shafique, and M. J. Mughal, "Polarization insensitive dual band frequency selective surface for RF shielding through glass windows," *IEEE Trans. Electromagn. Compat.*, vol. 62, no. 1, pp. 93–100, Feb. 2020, doi: 10.1109/TEMC.2019.2893408.

[86] B. Sanz-Izquierdo, J. B. Robertson, E. A. Parker, and J. C. Batchelor, "Small FSS arrays for indoor communications," in *Proc. IEEE Int. Workshop Antenna Technol., Small Antennas Novel Metamaterials*, Mar. 2008, pp. 466–469, doi: 10.1109/IWAT.2008.4511379.

[87] S. Ghosh and K. V. Srivastava, "Broadband polarization-insensitive tunable frequency selective surface for wideband shielding," *IEEE Trans. Electromagn. Compat.*, vol. 60, no. 1, pp. 166–172, Feb. 2018, doi: 10.1109/TEMC.2017.2706359.

[88] B. S. Abirami, E. F. Sundarsingh, and V. S. Ramalingam, "Mechanically reconfigurable frequency selective surface for RF shielding in indoor wireless environment," *IEEE Trans. Electromagn. Compat.*, vol. 62, no. 6, pp. 2643–2646, Dec. 2020, doi: 10.1109/TEMC.2020.2983899.

[89] J. F. de Lima, H. D. de Andrade, G. Fontgalland, A. S. B. Sombra, K. R. Lima, M. E. T. Sousa, and T. Silveira, "Study of current density and angular stability in frequency selective surfaces for indoor communications," in *IEEE MTT-S Int. Microw. Symp. Dig.*, Oct. 2021, pp. 1–3, doi: 10.1109/IMOC53012.2021.9624837.

[90] M. F. Imani, J. N. Gollub, O. Yurduseven, A. V. Diebold, M. Boyarsky, T. Fromenteze, L. Pulido-Mancera, T. Sleasman, and D. R. Smith, "Review of metasurface antennas for computational microwave imaging," *IEEE Trans. Antennas Propag.*, vol. 68, no. 3, pp. 1860–1875, Mar. 2020, doi: 10.1109/tap.2020.2968795.

[91] T. Sleasman, M. F. Imani, M. Boyarsky, K. P. Trofatter, and D. R. Smith, "Computational through-wall imaging using a dynamic metasurface antenna," *OSA Continuum*, vol. 2, no. 12, p. 3499, Dec. 2019, doi: 10.1364/osac.2.003499.

[92] S. S. Al-Bawri, M. T. Islam, T. Shabbir, G. Muhammad, M. S. Islam, and H. Y. Wong, "Hexagonal shaped near zero index (NZI) metamaterial based MIMO antenna for millimeter-wave application," *IEEE Access*, vol. 8, pp. 181003–181013, 2020, doi: 10.1109/ACCESS.2020.3028377.

[93] N. Zhang, W. X. Jiang, H. F. Ma, W. X. Tang, and T. J. Cui, "Compact high-performance lens antenna based on impedance-matching gradient-index metamaterials," *IEEE Trans. Antennas Propag.*, vol. 67, no. 2, pp. 1323–1328, Feb. 2019, doi: 10.1109/TAP.2018.2880115.

[94] K. Sun, S. Han, J. H. Choi, and J. K. Lee, "Miniaturized active metamaterial resonant antenna with improved radiation performance based on negative-resistance-enhanced CRLH transmission lines," *IEEE Antennas Wireless Propag. Lett.*, vol. 17, no. 7, pp. 1162–1165, Jul. 2018, doi: 10.1109/LAWP.2018.2836803.

[95] M. D. Banadaki, A. A. Heidari, and M. Nakhkash, "A metamaterial absorber with a new compact unit cell," *IEEE Antennas Wireless Propag. Lett.*, vol. 17, no. 2, pp. 205–208, Feb. 2018, doi: 10.1109/LAWP.2017.2780231.

[96] L. Li, H. Ruan, C. Liu, Y. Li, Y. Shuang, A. Alù, C.-W. Qiu, and T. J. Cui, "Machine-learning reprogrammable metasurface imager," *Nature Commun.*, vol. 10, no. 1, p. 1082, Mar. 2019, doi: 10.1038/s41467-019-09103-2.

[97] S. Abdullah, G. Xiao, and R. E. Amaya, "A review on the history and current literature of metamaterials and its applications to antennas & radio frequency identification (RFID) devices," *IEEE J. Radio Freq. Identificat.*, vol. 5, no. 4, pp. 427–445, Dec. 2021, doi: 10.1109/JRFID.2021.3091962.

[98] M. Pallavi, P. Kumar, T. Ali, and S. B. Shenoy, "Modeling of a negative refractive index metamaterial unit-cell and array for aircraft surveillance applications," *IEEE Access*, vol. 10, pp. 99790–99812, 2022, doi: 10.1109/access.2022.3206358.

[99] G. Gennarelli and G. Riccio, "On the accuracy of the uniform asymptotic physical optics solution for the diffraction by a PEC–DNG metamaterial junction," *IEEE Antennas Wireless Propag. Lett.*, vol. 19, no. 4, pp. 581–585, Apr. 2020, doi: 10.1109/LAWP.2020.2972308.

[100] U. C. Hasar and M. Bute, "Method for retrieval of electromagnetic properties of inhomogeneous reciprocal chiral metamaterials," *IEEE Trans. Antennas Propag.*, vol. 68, no. 7, pp. 5714–5717, Jul. 2020, doi: 10.1109/tap.2020.2979292.

[101] S. S. Bukhari, J. Vardaxoglou, and W. Whittow, "A metasurfaces review: Definitions and applications," *Appl. Sci.*, vol. 9, no. 13, p. 2727, Jul. 2019, doi: 10.3390/app9132727.

[102] Q. Lou and Z. N. Chen, "Sidelobe suppression of metalens antenna by amplitude and phase controllable metasurfaces," *IEEE Trans. Antennas Propag.*, vol. 69, no. 10, pp. 6977–6981, Oct. 2021, doi: 10.1109/TAP.2021.3076312.

[103] D. Kampouridou and A. Feresidis, "Tunable multibeam holographic metasurface antenna," *IEEE Antennas Wireless Propag. Lett.*, vol. 21, no. 11, pp. 2264–2267, Nov. 2022, doi: 10.1109/LAWP.2022.3192977.

[104] S. Vellucci, A. Monti, M. Barbuto, G. Oliveri, M. Salucci, A. Toscano, and F. Bilotti, "On the use of nonlinear metasurfaces for circumventing fundamental limits of mantle cloaking for antennas," *IEEE Trans. Antennas Propag.*, vol. 69, no. 8, pp. 5048–5053, Aug. 2021, doi: 10.1109/TAP.2021.3061010.

[105] O. M. Sanusi, Y. Wang, and L. Roy, "Reconfigurable polarization converter using liquid metal based metasurface," *IEEE Trans. Antennas Propag.*, vol. 70, no. 4, pp. 2801–2810, Apr. 2022, doi: 10.1109/TAP.2021.3137217.

[106] J. G. N. Rahmeier, T. J. Smy, J. Dugan, and S. Gupta, "Zero thickness surface susceptibilities and extended GSTCs—Part I: Spatially dispersive metasurfaces," *IEEE Trans. Antennas Propag.*, vol. 71, no. 7, pp. 5909–5919, Jul. 2023, doi: 10.1109/tap.2022.3164169.

[107] T. J. Smy, J. G. N. Rahmeier, J. Dugan, and S. Gupta, "Part II-spatially dispersive metasurfaces: IE-GSTC-SD field solver with extended GSTCs," *IEEE Trans. Antennas Propag.*, vol. 71, no. 7, pp. 5920–5934, Jul. 2023, doi: 10.1109/TAP.2022.3164125.

[108] C. Qi and A. M. H. Wong, "Discrete Huygens' metasurface: Realizing anomalous refraction and diffraction mode circulation with a robust, broadband and simple design," *IEEE Trans. Antennas Propag.*, vol. 70, no. 8, pp. 7300–7305, Aug. 2022, doi: 10.1109/TAP.2022.3164931.

[109] X. Meng, R. Liu, H. Chu, R. Peng, M. Wang, Y. Hao, and Y. Lai, "Through-wall wireless communication enabled by a metalens," *Phys. Rev. Appl.*, vol. 17, no. 6, Jun. 2022, Art. no. 064027, doi: 10.1103/physrevapplied.17.064027.

[110] R. Cicchetti, V. Cicchetti, A. Faraone, L. Foged, and O. Testa, "A compact high-gain wideband lens Vivaldi antenna for wireless communications and through-the-wall imaging," *IEEE Trans. Antennas Propag.*, vol. 69, no. 6, pp. 3177–3192, Jun. 2021, doi: 10.1109/TAP.2020.3037777.

[111] I. R. Gomes, B. S. L. Castro, R. L. Fraiha, H. S. Gomes, S. G. C. Fraiha, and G. P. S. Cavalcante, "Indoor propagation model in 2.4 GHz with QoS parameters estimation in VoIP calls, considering different types of walls and floors," in *Proc. 6th Eur. Conf. Antennas Propag. (EUCAP)*, Mar. 2012, pp. 2091–2094, doi: 10.1109/EuCAP.2012.6206494.

[112] W. H. Fan, L. Yu, Z. Wang, and F. Xue, "The effect of wall reflection on indoor wireless location based on RSSI," in *Proc. IEEE Int. Conf. Robot. Biomimetics (ROBIO)*, Dec. 2014, pp. 1380–1384, doi: 10.1109/ROBIO.2014.7090526.

[113] A. E. Shaikh, F. Majeed, M. Zeeshan, T. Rabbani, and I. Sheikh, "Efficient implementation of deterministic 3-D ray tracing model to predict propagation losses in indoor environments," in *Proc. 13th IEEE Int. Symp. Pers., Indoor Mobile Radio Commun.*, Sep. 2002, pp. 1208–1212, doi: 10.1109/PIMRC.2002.1045220.

[114] *Ground Penetrating Radar*. Accessed: 2022. [Online]. Available: http://iovasia.com/ground-penetrating-radar/

[115] Y. Pinhasi, A. Yahalom, and S. Petnev, "Propagation of ultra wide-band signals in lossy dispersive media," in *Proc. IEEE Int. Conf. Microw., Commun., Antennas Electron. Syst.*, May 2008, pp. 1–10.

[116] N. Qasem, "Enhancing wireless communication system performance through modified indoor environments," Doctoral dissertation, Loughborough Univ., Loughborough, U.K., 2014.

[117] S. S. Zhekov, O. Franek, and G. F. Pedersen, "Dielectric properties of common building materials for ultrawideband propagation studies [measurements corner]," *IEEE Antennas Propag. Mag.*, vol. 62, no. 1, pp. 72–81, Feb. 2020.

[118] Y. Cao, S. Dai, J. Labuz, and J. Pantelis, "Implementation of ground penetrating radar," Minnesota Dept. Transp., Local Road Res. Board, Univ. Minnesota Digit. Conservancy, Tech. Rep. DOT 2007-34, 2007. [Online]. Available: https://hdl.handle.net/11299/5588

[119] C. Amer-Yahia and T. Majidzadeh, "Inspection of insulated concrete form walls with ground penetrating radar," *Construct. Building Mater.*, vol. 26, no. 1, pp. 448–458, Jan. 2012.

[120] W. Zhang, A. Hoorfar, C. Thajudeen, and F. Ahmad, "Full polarimetric beam-forming algorithm for through-the-wall radar imaging," *Radio Sci.*, vol. 46, no. 5, pp. 1–17, Oct. 2011, doi: 10.1029/2010RS004631.

[121] V. N. Saxena, "Characterization of wall parameters and autofocusing techniques for through–the-wall-imaging system," in *Proc. Int. Conf. Signal Process. Commun. (ICSC)*, Dec. 2016, pp. 516–519, doi: 10.1109/ICSPCom.2016.7980635.

[122] D. Ferreira, T. R. Fernandes, R. F. S. Caldeirinha, and I. Cuinas, "Characterization of wireless propagation through traditional Iberian brick walls," in *Proc. 11th Eur. Conf. Antennas Propag. (EUCAP)*, Mar. 2017, pp. 2454–2458, doi: 10.23919/EuCAP.2017.7928372.

[123] S. Magoon and A. E. Fathy, "Compact monostatic/bistatic UWB radar for wall characterization," in *Proc. IEEE Benjamin Franklin Symp. Microw. Antenna Sub-Syst. Radar, Telecommun., Biomed. Appl. (BenMAS)*, Sep. 2014, pp. 1–3, doi: 10.1109/BenMAS.2014.7529457.

[124] A. Muqaibel and A. Safaai-Jazi, "Characterization of wall dispersive and attenuative effects on UWB radar signals," *J. Franklin Inst.*, vol. 345, no. 6, pp. 640–658, Sep. 2008, doi: 10.1016/j.jfranklin.2008.01.002.

[125] B. A. Nia, S. Sadeghi, and F. De Flaviis, "Using the convolutional neuron network for target localization and wall characterization in the through the wall imaging problem," in *Proc. 16th Eur. Conf. Antennas Propag. (EuCAP)*, Mar. 2022, pp. 1–3.

[126] I. Vilovic, N. Burum, and R. Nadj, "Estimation of dielectric constant of composite materials in buildings using reflected fields and PSO algorithm," in *Proc. 4th Eur. Conf. Antennas Propag.*, Apr. 2010, pp. 1–5.

[127] I. Vilovic, R. Nad, Z. Sipus, and N. Burum, "A non-destructive approach for extracting the complex dielectric constant of the walls in building," in *Proc. 50th Int. Symp. (ELMAR)*, Sep. 2008, pp. 609–612.

[128] C. Thajudeen, A. Hoorfar, and W. Zhang, "Estimation of frequency-dependent parameters of unknown walls for enhanced through-the-wall imaging," in *Proc. IEEE Int. Symp. Antennas Propag. (APSURSI)*, Jul. 2011, pp. 3070–3073.

[129] W. Zhang and A. Hoorfar, "Three-dimensional real-time through-the-wall radar imaging with diffraction tomographic algorithm," *IEEE Trans. Geosci. Remote Sens.*, vol. 51, no. 7, pp. 4155–4163, Jul. 2013.

[130] C. Thajudeen and A. Hoorfar, "A hybrid bistatic–monostatic radar technique for calibration-free estimation of lossy wall parameters," *IEEE Antennas Wireless Propag. Lett.*, vol. 16, pp. 1249–1252, 2017.

[131] M. Aftanas, J. Sachs, M. Drutarovský, and D. Kocur, "Efficient and fast method of wall parameter estimation by using UWB radar system," *Frequenz*, vol. 63, nos. nos. 11–12, pp. 231–235, Jan. 2009.

[132] S. Sadeghi, K. Mohammadpour-Aghdam, K. Ren, R. Faraji-Dana, and R. J. Burkholder, "A pole-extraction algorithm for wall characterization in through-the-wall imaging systems," *IEEE Trans. Antennas Propag.*, vol. 67, no. 11, pp. 7106–7113, Nov. 2019, doi: 10.1109/TAP.2019.2927870.

[133] M. Lott and I. Forkel, "A multi-wall-and-floor model for indoor radio propagation," in *Proc.IEEE VTS 53rd Veh. Technol. Conf., Spring*, May 2001, pp. 464–468, doi: 10.1109/VETECS.2001.944886.

[134] Y. Liu, K. A. Hassan, M. Karlsson, O. Weister, and S. Gong, "Active plant wall for green indoor climate based on cloud and Internet of Things," *IEEE Access*, vol. 6, pp. 33631–33644, 2018, doi: 10.1109/ACCESS.2018.2847440.

[135] IEEE 802 LAN/MAN Standards Committee. (2009). *Wireless LAN Media Access Control (MAC) and Physical Layer (PHY) Specifications*. [Online]. Available: http://standards.ieee.org/getieee802/

[136] S. Kutty and D. Sen, "Beamforming for millimeter wave communications: An inclusive survey," *IEEE Commun. Surveys Tuts.*, vol. 18, no. 2, pp. 949–973, 2nd Quart., 2016.

[137] T. Manabe, Y. Miura, and T. Ihara, "Effects of antenna directivity on indoor multipath propagation characteristics at 60 GHz," in *Proc. 6th Int. Symp. Pers., Indoor Mobile Radio Commun.*, Sep. 1985, p. 1035.

[138] T. Manabe, Y. Miura, and T. Ihara, "Effects of antenna directivity and polarization on indoor multipath propagation characteristics at 60 GHz," *IEEE J. Sel. Areas Commun.*, vol. 14, no. 3, pp. 441–448, Apr. 1996.

[139] A. Maltsev, R. Maslennikov, A. Maltsev, A. Khoryaev, and M. Shilov, "Performance analysis of spatial reuse mode in millimeter-wave WPAN systems with multiple links," in *Proc. IEEE 19th Int. Symp. Pers., Indoor Mobile Radio Commun.*, Sep. 2008, pp. 1–4.

[140] Z. Genc, U. H. Rizvi, E. Onur, and I. Niemegeers, "Robust 60 GHz indoor connectivity: Is it possible with reflections?" in *Proc. IEEE 71st Veh. Technol. Conf.*, May 2010, pp. 1–5.

[141] M. Park and H. K. Pan, "A spatial diversity technique for IEEE 802.11 ad WLAN in 60 GHz band," *IEEE Commun. Lett.*, vol. 16, no. 8, pp. 1260–1262, 2012.

[142] C. Yiu and S. Singh, "Empirical capacity of mmWave WLANS," *IEEE J. Sel. Areas Commun.*, vol. 27, no. 8, pp. 1479–1487, Oct. 2009.

[143] S. Pisa, E. Piuzzi, E. Pittella, P. D'Atanasio, A. Zambotti, and G. Sacco, "Comparison between delay and sum and range migration algorithms for image reconstruction in through-the-wall radar imaging systems," *IEEE J. Electromagn., RF Microw. Med. Biol.*, vol. 2, no. 4, pp. 270–276, Dec. 2018, doi: 10.1109/JERM.2018.2878070.

[144] K. Wang, Z. Zeng, and J. Sun, "Through-wall detection of the moving paths and vital signs of human beings," *IEEE Geosci. Remote Sens. Lett.*, vol. 16, no. 5, pp. 717–721, May 2019, doi: 10.1109/LGRS.2018.2881311.

[145] D. Yang, Z. Zhu, J. Zhang, and B. Liang, "The overview of human localization and vital sign signal measurement using handheld IR-UWB through-wall radar," *Sensors*, vol. 21, no. 2, p. 402, Jan. 2021, doi: 10.3390/s21020402.

[146] Z. Guo, F. Xiao, B. Sheng, L. Sun, and S. Yu, "TWCC: A robust through-the-wall crowd counting system using ambient WiFi signals," *IEEE Trans. Veh. Technol.*, vol. 71, no. 4, pp. 4198–4211, Apr. 2022, doi: 10.1109/TVT.2022.3140305.

[147] *Characteristics of Ultra Wideband Technology*, document ITU 1755, ITU-R SMR, 2006.

[148] C. A. Balanis, *Antenna Theory: Analysis and Design*. Hoboken, NJ, USA: Wiley, 2015.

[149] M. Chinthavali, "3D printing technology for automotive applications," in *Proc. Int. Symp. 3D Power Electron. Integr. Manuf. (3D-PEIM)*, Jun. 2016, pp. 1–13, doi: 10.1109/3DPEIM.2016.7570535.

[150] Y. Xiong and Z. Qu, "Antenna 3D pad printing solution evaluation," in *Proc. IEEE Int. Symp. Antennas Propag. (APSURSI)*, Jul. 2011, pp. 2773–2776, doi: 10.1109/APS.2011.5997101.

[151] X. He and M. M. Tentzeris, "A 3D printed dish antenna with integrated feeding structure," in *Proc. IEEE Int. Symp. Antennas Propag. North Amer. Radio Sci. Meeting*, Jul. 2020, pp. 1603–1604, doi: 10.1109/IEEECONF35879.2020.9329541.

[152] M. F. Farooqui and A. Kishk, "3-D-printed tunable circularly polarized microstrip patch antenna," *IEEE Antennas Wireless Propag. Lett.*, vol. 18, no. 7, pp. 1429–1432, Jul. 2019, doi: 10.1109/LAWP.2019.2919255.

[153] S. Dogu, I. Dilman, A. O. Ertay, and A. Uysal, "Modified printed monopole antenna with well-matched impedance bandwidth for through the wall microwave imaging applications," in *Proc. 28th Telecommun. Forum (TELFOR)*, Nov. 2020, pp. 1–4, doi: 10.1109/TELFOR51502.2020.9306657.

[154] M. Czelen, M. Rzymowski, K. Nyka, and L. Kulas, "Miniaturization of ESPAR antenna using low-cost 3D printing process," in *Proc. 14th Eur. Conf. Antennas Propag. (EuCAP)*, Mar. 2020, pp. 1–4.

[155] B. Sanz-Izquierdo and E. A. Parker, "3D printed FSS arrays for long wavelength applications," in *Proc. 8th Eur. Conf. Antennas Propag. (EuCAP)*, Apr. 2014, pp. 2382–2386, doi: 10.1109/EuCAP.2014.6902296.

[156] R. Kronberger and V. Wienstroer, "3D-printed FSS using printing filaments with enclosed metal particles," in *Proc. Prog. Electromagn. Res. Symp. Fall (PIERS-FALL)*, Nov. 2017, pp. 808–811.

HOJJAT JAMSHIDI-ZARMEHRI (Graduate Student Member, IEEE) received the bachelor's degree in electrical engineering from the University of Birjand, Birjand, Iran, in 2012, and the master's degree in electrical engineering from the Ferdowsi University of Mashhad, Mashhad, Iran, in 2018. He is currently pursuing the Ph.D. degree with Carleton University, Ottawa, Canada, where he is working on the design and development of antennas and other microwave components for millimeter wave applications.

AMIR AKBARI was born in Iran, in 1985. He received the B.Sc. degree from Qazvin Islamic Azad University, Qazvin, Iran, in 2010, and the M.Sc. degree in electrical and electronics engineering from the Amir Kabir University of Technology (Tehran Polytechnic), Tehran, Iran, in 2013. He is currently pursuing the Ph.D. degree with the Electrical Engineering Department, Carleton University, Ottawa, Canada. He was a Lecturer with Karaj Islamic Azad University, Karaj, Iran, from 2014 to 2021. His research interests include electromagnetic theory, antennas, microwave, and millimeter wave circuits.
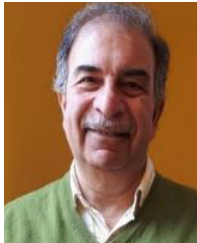
MOHAMMAD LABADLIA was born in Guelma, Algeria, in 1992. He received the master's degrees in electronics systems from the University of Guelma, Guelma, and in microwave/optical electronics from the University of Limoges, Limoges, France, in 2016 and 2019, respectively. He is currently pursuing the Ph.D. degree in electrical and computer Engineering with Carleton University, Ottawa, Canada. His research interests include tunable materials as applied to antenna systems, FSS, metasurfaces, metalenses and the analysis of through the wall communication problems.

KAM EUCHARIST KEDZE received the Bachelor of Technology degree in electrical and electronic engineering (telecommunication) from the University of Buea, Buea, Cameroon, in 2013, and the M.S. degree in electrical and computer engineering from Ajou University, Suwon, South Korea, in 2019. He is currently pursuing the Ph.D. degree with the Department of Electronics, Carleton University, Ottawa, Canada. His research interests include the design of active and reconfigurable antennas and metamaterials for active electronically scanned arrays.

JAFAR SHAKER (Senior Member, IEEE) received the B.Sc. degree in electrical engineering from the Iran University of Science and Technology, Tehran, Iran, in 1987, and the Ph.D. degree from the University of Manitoba, Winnipeg, MB, Canada, in 1995. He was a Research Scientist with the Communications Research Center, Ottawa, ON, Canada, from 1996 to 2022. He is currently an Adjunct Professor with the Department of Electronics, Carleton University, Ottawa. He has authored or coauthored more than 200 technical articles in journals and conference proceedings. His current research interests include periodic structures, reflectarray, frequency selective surfaces (FSS), quasi-optical techniques, electromagnetic band-gap structures, leaky-wave antennas, and the application of optical concepts in microwave and antenna engineering.

GAOZHI (GEORGE) XIAO (Fellow, IEEE) received the Ph.D. degree from Loughborough University, U.K., in 1995. He has worked in industries, academics, and government labs. His expertise covers multi-disciplinary fields, including the IoT, flexible/printable/wearable electronics, fiber optic sensor systems, structural health monitoring, and structural materials. He was awarded the 2014 Technical Award and the 2018 Distinguished Service Award by the IEEE Instrumentation and Measurement Society. He was a recipient of 2022 Edison Award for materials breakthrough in the category of consumer solutions and the 2022 Research and Development 100 Award. He is a fellow of the Engineering Institute of Canada and a Principle Research Officer at the National Research Council Canada.

RONY E. AMAYA (Senior Member, IEEE) received the M.Eng. and Ph.D. degrees from Carleton University, Ottawa, ON, Canada, in 2001 and 2005, respectively. He joined the Design Center, Skyworks Solutions, Ottawa, in 2003. He was involved in the design of RFIC's for wireless transceivers. He was a Research Scientist with the Communications Research Centre Canada, from 2006 to 2015, developing research and development technology for integrated RF circuit and system solutions from S-band to E-band and addressing packaging and antenna integration. He currently manages research programs in collaboration with the National Research Council (NRC), Skyworks, Nanowave Technologies, ELPHIC, and Cienna. He joined the Department of Electronics, Carleton University, as an Associate Professor, in 2016. His research interests include RF system design, MMICs and packaging for high-frequency and high-speed applications, active antennas and metamaterials, and energy harvesting and wireless power transfer. He has authored or coauthored more than 120 technical articles in journals and conference proceedings and holds several patents. He is a member of the Association of Professional Engineers of Ontario.

● ● ●